A Class of Compact Substrate Integrated Waveguide Filters

Chandra Sekhar Panda

Department of Electronics and Communication Engineering
National Institute of Technology Rourkela

A Class of Compact Substrate Integrated Waveguide Filters

Thesis submitted in partial fulfillment

of the requirements of the degree of

Master of Technology

in

Electronics and Communication Engineering
(*Specialization*: *Communication and Networks*)

by

Chandra Sekhar Panda

(Roll Number: 214EC5218)

based on research carried out

under the supervision of

Prof. Santanu Kumar Behera

May, 2016

Department of Electronics and Communication Engineering
National Institute of Technology Rourkela

Department of Electronics and Communication Engineering
National Institute of Technology Rourkela

Prof. Santanu Kumar Behera
Associate Professor

May 30, 2016

Supervisor's Certificate

This is to certify that the work presented in the dissertation entitled *A Class of Compact Substrate Integrated Waveguide Filters* submitted by *Chandra Sekhar Panda*, Roll Number 214EC5218, is a record of original research carried out by him under my supervision and guidance in partial fulfillment of the requirements of the degree of *Master of Technology* in *Electronics and Communication Engineering*. Neither this thesis nor any part of it has been submitted earlier for any degree or diploma to any institute or university in India or abroad.

_____
Santanu Kumar Behera

Dedication

I dedicate this work to my beloved papa, mommy and friends.

Signature

Declaration of Originality

I, *Chandra Sekhar Panda*, Roll Number *214EC5218* hereby declare that this dissertation entitled *A Class of Compact Substrate Integrated Waveguide Filters* presents my original work carried out as a postgraduate student of NIT Rourkela and, to the best of my knowledge, contains no material previously published or written by another person, nor any material presented by me for the award of any degree or diploma of NIT Rourkela or any other institution. Any contribution made to this research by others, with whom I have worked at NIT Rourkela or elsewhere, is explicitly acknowledged in the dissertation. Works of other authors cited in this dissertation have been duly acknowledged under the sections "Reference" or "Bibliography". I have also submitted my original research records to the scrutiny committee for evaluation of my dissertation.

I am fully aware that in case of any non-compliance detected in future, the Senate of NIT Rourkela may withdraw the degree awarded to me on the basis of the present dissertation.

May 30, 2016
NIT Rourkela

Chandra Sekhar Panda

Acknowledgement

I would like to thank my advisor, Professor S. K. Behera, for his excellent guidance and support throughout the whole project work and writing of this thesis. He has motivated me to be creative, taught the ethics of research and the skills to present ideas in front of others.

I would also like to express my sincere gratitude to our HOD Prof. K. K. Mahapatra for providing excellent Laboratory facilities throughout this work. I would like to thank all the Faculty Members of Electronics and Communication department, especially of the Communication group for their constant support and encouragement.

I am also grateful to Rashmiranjan, all friends and colleagues for their support and for being actively involved in each and every steps of this project work. The discussions were very helpful throughout this work.

Finally, I would like to thank my parents who have always been very supportive and understanding throughout my life.

May 30, 2016
NIT Rourkela

Chandra Sekhar Panda
Roll Number: 214EC5218

Abstract

This thesis work explores the design of compact and high performance microwave filters using substrate integrated waveguide technology. A substrate integrated waveguide is a planar version of a conventional waveguide, which is having features like planar circuit integrability, ease of fabrication, low-cost and high power handling. A class of Substrate Integrated Waveguide (SIW) and Half mode Substrate Integrated waveguide (HMSIW) bandpass filters are proposed in this context. Applications like satellite communication uses devices which can withstand high power. Therefore, SIW filters can be used for satellite applications in the microwave bands like Ku, X, C, S, and L etc.

The main objective of this thesis is to design SIW bandpass filters using simple planar technology and low-cost substrates. To fulfill this, a class of compact and easily fabricable SIW bandpass filters are proposed for Ku-band ($12 - 18GHz$) and S-band ($2 - 4GHz$) applications. These filters are designed using simple electromagnetic band gap (EBG) structures and latest feeding techniques like tapered-via feeding. Filters are designed using low-cost and easily available substrate FR4 with the help of High frequency structural simulator (HFSS) V.14. The dimensions of the filters are optimized and simulation results are analyzed. The proposed Ku-band filter has proven to be compact since its footprint is $160mm^2$. The S-band filter has been fabricated using low-cost and easily available FR4 substrate. The measurement results are found to be good in agreement with the simulation results. Though the obtained results are similar to the other reported filters, there is a huge demand of compactness in this miniaturization era. Therefore, another well-established concept of Half-mode SIW (HMSIW) technology is used to further reduce the size of the designed filters. So a compact HMSIW bandpass filter is designed for the Ku-band applications which is almost half in size as compared to conventional SIW designs. The return loss is achieved as $45dB$ and insertion loss is $1.5dB$ in the passband of the filter, which is promising corresponding to the size. Another similar design is made for X-band ($8 - 12GHz$) applications using HMSIW technology. The overall footprint of the filter which shows its compactness; is $102mm^2$ i.e. almost half the size of its equivalent SIW filter.

Keywords*: *SIW*; *HMSIW*; *EBG*; *HFSS*; *Ku-band.

Contents

List of Figures

List of Tables

Chapter 1

INTRODUCTION

In the recent years, the use of microwave filters has been increased to manifolds because of its applications in satellite communications, electronic warfare systems, military radar and TV broadcasting systems. A microwave filter is a frequency selective network normally working in the microwave frequency range i.e. from 300MHz-300GHz which allows the signals to transmit in the passband and provides high attenuation in the stopband of the filter. Since the demand for compact and high fidelity communication systems are increased, hence many technologies for microwave filter design are developed. One such famous technology is Substrate Integrated Waveguide (SIW) technology.

Substrate integrated waveguide technology has been an emerging field of research in the recent years. Since it possess some special characteristics such as low-cost, relatively low-loss, high Quality, ease of fabrication and mass-production which is considered to be the best of both conventional waveguides as well as the planar microstrip structures. One such comparison between the planar microstrip structure and conventional waveguide is shown in Figure 1.1. The performance gap is bridged using SIW as shown in the Figure 1.1. These characteristics also allow a user to improve the bandwidth and size of the microwave component without losing its performance.

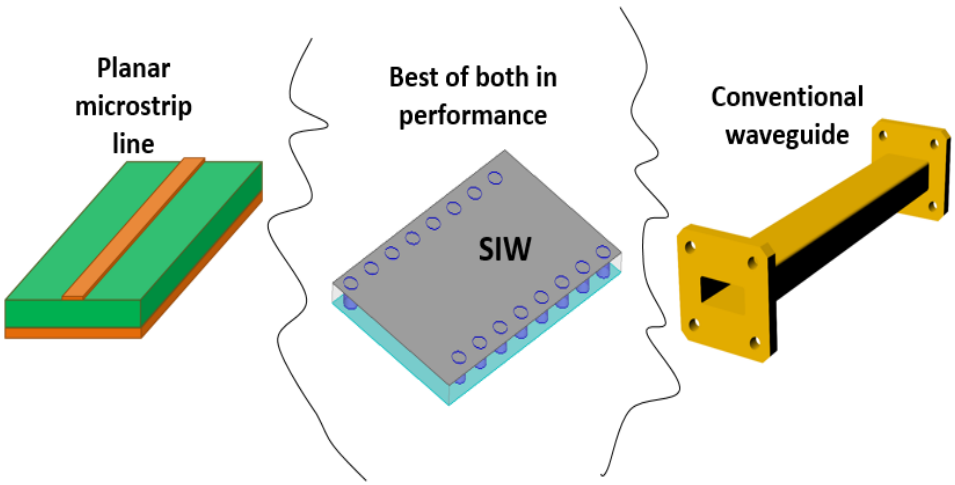

Figure 1.1: Performance gap diagram of waveguide and planar structure

Microwave filters are devices which can separate the wanted frequencies from unwanted frequencies [1-4]. Substrate Integrated Waveguide (SIW) is the technology used to design high power handling and planar integrable devices such as isolators, filters, power dividers and couplers [5]. A detailed study of fundamentals about SIW has been presented in [5, 6]. In the process of designing a SIW bandpass filter the width of it plays an important role. A new formula for effective width calculation has been described in [7]. Transition between SIW and other planar devices are very much required to provide excitation to these structures. One such wideband transition from microstrip to SIW is proposed in [8]. A number of slotted topologies using the electromagnetic band-gap (EBG) structures are presented in [9-11]. In these proposed designs the basic EBG structure is a U-slot. Guided-wave analysis, leakage characteristics, accurate modelling and wave mechanism of a SIW are described in [12-13]. Design methodology of SIW filter and its dispersion characteristics are presented in [14, 15]. Since there is a mismatch in the impedance of the microstrip line and the SIW, the transitions are required to provide matching as described in [16, 17]. Half-mode geometries are possible due to the magnetic wall behavior shown by the symmetric plane along the direction of propagation. Such geometries are proposed in [18, 19].

1.1 Motivation

Though many technologies are there to design microwave filters, SIW seems promising because of its qualities like high power handling, planar structure, easy fabrication and ease of integration with other planar antennas. But still there is sufficient scope for the development in these filters for miniaturized applications. Due to the multiplexing applications in wireless communication channels the demand for sharp cutoff frequency filters have been increased. Therefore, in this thesis the filters for different microwave frequency bands are proposed using latest advancements in the SIW like the use of Electromagnetic band-gap (EBG) structures and better feeding mechanisms to improve the overall performance of the filters. So this motivates to design SIW filters with following requirements:

- Design of a compact SIW bandpass filter with high isolation and low-reflection.
- Design of SIW filters with linear performance in the passband with very low and constant group delay.
- SIW filter design with wideband and sharp transition response.

1.2 Objective

The objective of this work is to design a class of compact SIW bandpass filters. The filters are to be designed to work in Ku, X and S bands of the microwave frequencies. The objective can be specified as follows:

- Design of a compact SIW filter for Ku-band applications.
- Design of a half-mode SIW (HMSIW) filter for X-band and Ku-band applications.

1.3 Contribution

- A compact and improved Ku band bandpass filter with a smooth planar microstrip to SIW transition having multiple 'U'-slots is designed. In this Size is reduced by at least two times as compared to the other traditional filters operating in Ku-band.
- A half-mode SIW bandpass filter is proposed for X-band (8-12GHz) applications. Size of the designed X-band HMSIW filter is reduced by 50% in terms of its width as compared to other SIW filters for similar applications.
- Another S-band (2-4GHz) SIW filter is designed and fabricated using low-cost and widely available substrate FR4.
- Designs are simple using EBG structures to provide better stopband response.
- Lower group delay of around 0.2 nanosec in all the designs which shows the linearity of the filter response.

1.4 Structure of thesis

This thesis explores the design of compact and high performance microwave filters using substrate integrated waveguide (SIW) and half-mode SIW (HMSIW) technology. A class of Substrate Integrated Waveguide (SIW) bandpass filters for different microwave bands are proposed in this context. The work in this thesis are divided into the following chapters.

Chapter 2 describes about the various types of microwave filters, filter basics and their design methodology. This also includes the literature survey of latest trends and techniques to microwave filter design for the applications like satellite communication, millimeter-wave and others. Out of which an exhaustive study is carried out for SIW filters.

Chapter 3 is about the design and analysis of SIW bandpass filters for Ku-band and S-band applications using Electromagnetic Band-gap (EBG) structures. It also includes the latest feeding techniques like tapered-via feeding for better passband performance of the filters.

Parametric study is used to get the best dimensions for the proposed bandpass filters and making them compact. The designs were made using high frequency structural simulator (HFSS) V.14.

Chapter 4 presents a study of HMSIW (Half mode SIW) filters by designing X-band and Ku-band bandpass filters using Half-mode concept. Half-mode structures show an excellent gain in the footprint of the filter circuit by reducing the size to half of its original size without losing the performance.

Chapter 5 summarizes the work done in this thesis by providing brief conclusions and the future scope for the project.

Chapter 2

Substrate Integrated Waveguide Filters

2.1 Introduction

In this chapter, a brief overview of microwave filters are presented. The basic fundamentals of microwave filter design and the performance parameters are also discussed. Except that the other things which are presented includes rectangular waveguide, Substrate Integrated Waveguide (SIW) and the relation between these two. Though many things are covered in this chapter related to SIW technology but main focus is given to the SIW filter design process.

2.2 Microwave Filters

A microwave filter is a frequency selective network generally working in the microwave frequency range i.e. from 300MHz-300GHz which allows good transmission of signals in the passband and provides high attenuation in the stopband of the filter [1-4]. The various types of frequency selectivity achieved by employing these filters are lowpass, highpass, bandpass and bandstop. Microwave filters play a vital role in the electronic systems, communications systems such as mobile communication, satellite and radar systems [2]. In cellular communication very specific requirements needs to be followed in base station as well as in cellphones. In the Figure 2.1 such an instance is shown which shows a block diagram of a RF front-end of the cellular base station.

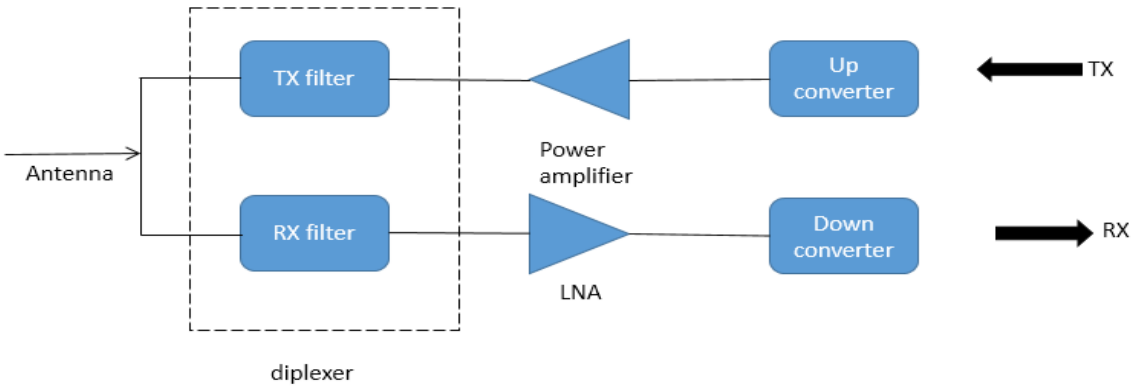

Figure 2.1: Block diagram of a RF front end of a mobile base station [2]

The antenna shown in Figure 2.1 works as a transceiver. So while transmitting the signal the receiving filter needs to provide very high attenuation for the signals in the transmission band and should also follow the criteria of low insertion loss in the passband. Since there are some strict means needs to be taken care of while designing microwave filters, hence comes the filter design methods. Although there exists a number of methods and technologies to design microwave filters, the miniaturization and efficiency characteristics are still a challenging problem.

2.3 Filter Design Methods

2.3.1 Performance characteristics

The performance of a microwave filter is characterized by certain factors like insertion loss, return loss, quality factor (Q-factor), group delay and fractional or 3dB bandwidth. However these are not the only parameters considered while designing a filter. In the following section a brief description of these factors are presented.

a. Insertion loss

The loss in the signal power due to the insertion of a microwave device or transmission line is called insertion loss. Its mathematical relation with the transmission coefficient (τ) is given in the following Eq. (2.1).

$$\text{IL} = 10\log\left(\frac{P_T}{P_R}\right) = -20\log|\tau| \tag{2.1}$$

where P_T and P_R denotes the transmitted and received power respectively.

b. Return loss

The loss in the incident power due to the impedance mismatching is called return loss of the filter as in [2]. It's symbolized as:

$$\text{RL} = 10\log\left(\frac{P_i}{P_r}\right) = -20\log|\Gamma| \tag{2.2}$$

where P_i and P_r denotes the incident and reflected power respectively. Where Γ denotes the reflection coefficient of the filter.

c. Group delay

Group delay shows the presence of linearity in the filter response. If the group delay provided by the filter is constant, then the phase response of the filter is said to be linear. It can be denoted as:

$$\tau_g = -\frac{d\psi(\omega)}{d\omega} \tag{2.3}$$

where $\psi(\omega)$ represents the phase response of the filter and for a constant group delay this has to follow linearity [2].

i.e. $$\psi(\omega) = k\omega \tag{2.4}$$

where k is a constant and ω is the angular frequency in rads/sec.

d. Fractional bandwidth

Fractional bandwidth (FBW) of a bandpass filter can be defined as the ratio of the filter bandwidth to its center frequency. It's normally used to categorize between wideband and ultra wideband (UWB) filters. If FBW is greater than 0.25 or 25% then the filter response is said to be UWB in nature.

$$\text{FBW} = \frac{f_2 - f_1}{f_c} \tag{2.5}$$

where f_c is the center frequency; f_1 and f_2 are the lower and upper cutoff frequencies respectively.

Apart from this there are other factors like Quality factor, radiation loss, efficiency etc., which are also important while doing the study of a microwave filter. These aspects are termed in the following chapters.

2.3.2 Filter design process

The strict requirements of communication systems lead to the invention of many techniques of filter design. Some of these famous techniques are image parameter method and insertion loss method [4]. In image parameter method, an equivalent two port network is formed using LC sections for providing a filtered response. However, the analysis is not very flexible for producing specific frequency response over the range. The later one, i.e. the insertion loss method uses network synthesis for designing a filter to get the desired response. This method is comparatively easier as compared to image-parameter method, since it starts with a low

pass model and then that is converted to its equivalent high-pass or band-pass model by using frequency and impedance transformations.

(i) Determination of the transfer function

Generally the transfer function of the filter is approximated using Butterworth, Chebyshev and elliptic functions as in [4].

The Butterworth gives the simplest approximation for an ideal low-pass filter which is maximally flat in nature [2]:

$$|S_{12}\,(j\omega)|^2 = \frac{1}{1+\omega^{2N}} \tag{2.6}$$

Therefore the insertion loss is given as

$$L_A = 10\log_{10}(1+\omega^{2N}) \tag{2.7}$$

where $S_{12}(j\omega)$ is transmission coefficient.

Where ω denotes the angular frequency and N corresponds to the degree of the network. At "w=1rad/sec" the insertion loss becomes 3-dB, hence this is known as the cut-off frequency of the filter i.e. ω_c =1 rad/sec. This cutoff also marks the transition between the passband and stopband of the response. As the value of N i.e. the order of the filter increases the transition becomes sharp and faster.

The return loss can be obtained using the Eq. (2.8) as given below:

$$|S_{11}(j\omega)|^2 = \frac{\omega^{2n}}{\omega^{2n}+1} \tag{2.8}$$

Where $S_{11}(j\omega)$: reflection coefficient

Another widely used attenuation characteristic is the "*Tchebyscheff*" or equi-ripple function. The scattering parameters related to this response can be defined considering $T(\omega)$ as the chebyshev function of order n are as follows:

$$|S_{11}(\omega)|^2 = \frac{1}{1+\epsilon^2 T^2(\omega)} \tag{2.9}$$

$$|S_{21}(\omega)|^2 = \frac{T^2(\omega)}{1+\epsilon^2 T^2(\omega)} \tag{2.10}$$

where ϵ is the ripple constant corresponds to the ripples present in the passband of the filter.

Thus from Eq. (2.10) the insertion loss can be calculated as:

$$L_A(\omega) = 10\log_{10}(1 + \epsilon^2 T^2(\omega)) \quad (2.11)$$

The attenuation characteristics for a low pass prototype filter has been presented in the Figure 2.2 from [1].

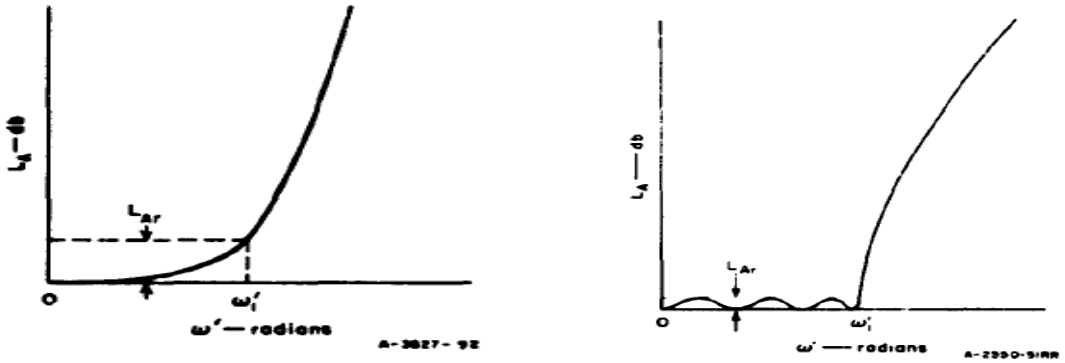

(a) (b)

Figure 2.2: (a) Butterworth lowpass characteristics (b) Chebyshev lowpass characteristics [1]

It can be observed from the Figure 2.2 that, though the Butterworth provides maximally flat response in the passband but the transition to stopband is very slow as compared to chebyshev characteristics. For sharp cutoff frequency requirements, chebyshev will be the best choice but the passband ripples will have some effect on the input signal.

(ii) Lumped network transformations

Most of the microwave filters work in a 50Ω environment, therefore 1Ω impedance level needs to be scaled to 50 Ω (Z_0) impedance level. That's the reason for impedance scaling. In case of an inductor the value gets multiplied by Z_0 and in case of a capacitor it gets divided by the same. This can be written as following [2]:

$\mathrm{L} \Rightarrow Z_0\mathrm{L}$ and $\mathrm{C} \Rightarrow \mathrm{C}/Z_0$

a. Lowpass to lowpass for arbitrary cutoff frequency

The cutoff frequency of a lowpass prototype is basically 1Hz. The transformation needed to convert this to any random frequency of ω_c is described in this section.

Consider a lowpass transmission characteristic of the type

$$|S_{12}\,(j\omega)|^2 = \frac{1}{1+F_N^2(\omega)} \tag{2.12}$$

After the frequency transformation from ω to $\omega/\,\omega_c$ we get the cutoff frequency at ω_c .

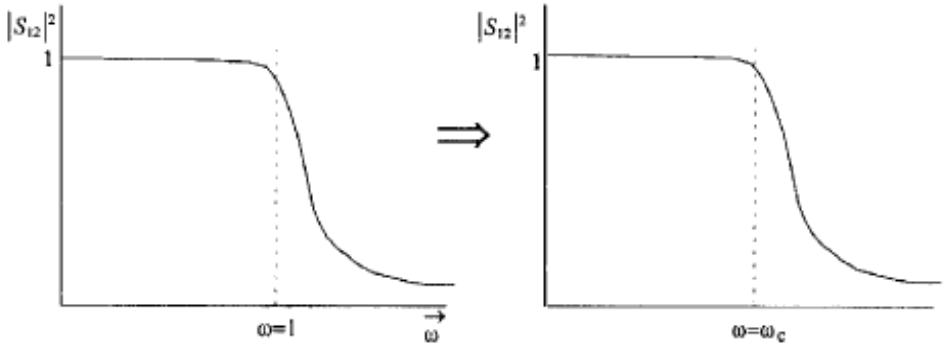

Figure 2.3 lowpass to lowpass transformation [2]

The element or network components are also transformed as given in Figure 2.4 using description given in [2].

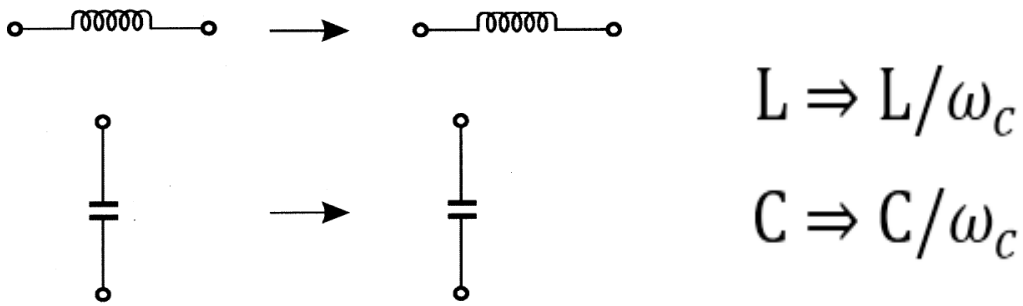

Figure 2.4: Element transformations for lowpass

b. Lowpass to highpass transformation

The transformation for frequency is

$$\omega \Rightarrow \frac{-\omega_c}{\omega} \tag{2.13}$$

The element transformation can be similarly presented in the Figure 2.5.

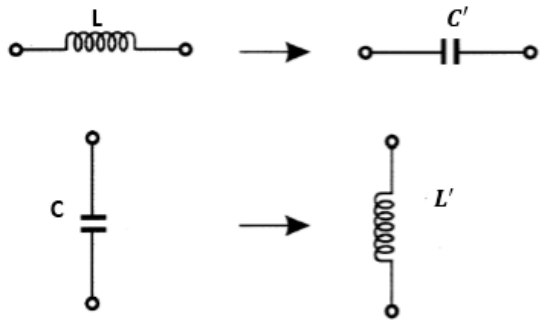

$$C' = \frac{1}{\omega_c L}$$

$$L' = \frac{1}{\omega_c C}$$

Figure 2.5: Element transformations for lowpass-highpass

The other transformations like lowpass to bandpass and lowpass to bandstop can be done in the similar approach. Though many techniques are present, but Substrate integrated waveguide technique became very famous in these days due to its performance characteristics and ease of fabrication. In the next section a literature survey of SIW technology is presented.

2.4 Substrate Integrated Waveguide

2.4.1 Waveguide

A waveguide is a hollow or dielectric filled metallic tube with uniform cross sections used to direct the electromagnetic wave by confining the energy. Waveguide is bulky and expensive but has the capability of high power handling [4] and low-loss. The use of planar microwave structures like microstrip lines and striplines has become more common these days due to the requirements for portable devices and miniaturization of communication systems, however the need for low-loss and high power handling structures like waveguides has not been ignored. The applications of waveguides are frequent in satellite systems and millimeter wave structures.

(i) Rectangular waveguide

A waveguide having rectangular cross section is called as a rectangular waveguide (RWG). A substrate integrated waveguide follows the working principle of a rectangular waveguide. The structure of the rectangular waveguide is shown in Figure 2.6 where it's considered that the guide is filled with dielectric material of permittivity ϵ and permeability μ . Maxwell's field equations are used to find the electromagnetic field configurations exist in a rectangular waveguide. Transverse electric (TE) and transverse magnetic(TM) modes are present in a rectangular waveguide. TEM, i.e. transverse electromagnetic mode doesn't present in a

RWG since TEM requires two conductors to propagate. *TE* and *TM* modes are generally denoted as TE_{mn} and TM_{mn} , where m and n corresponds to the mode numbers.

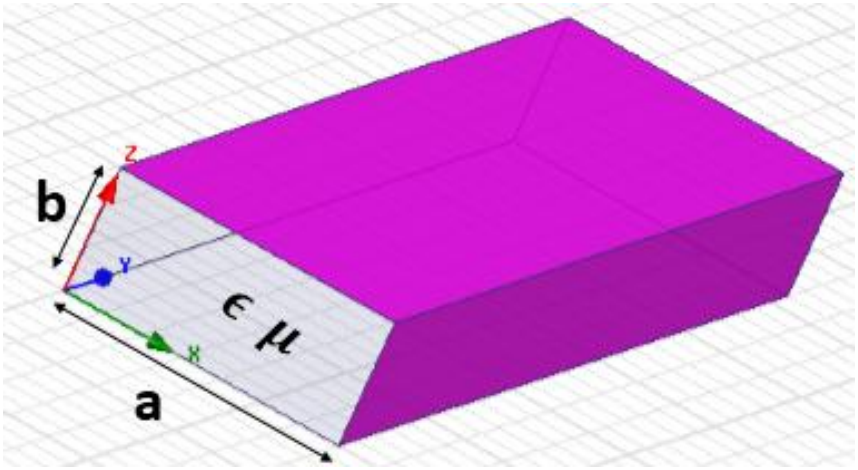

Figure 2.6 Geometry of a Rectangular waveguide

a. TE Modes

The structure of the rectangular waveguide is shown in Figure 2.6 where it's considered that the guide is filled with dielectric material of permittivity ϵ and permeability μ . For the TE mode the electric field component along the direction of propagation becomes zero (E_z=0). The Maxwell's equations and boundary conditions of electric and magnetic fields are used to derive the field components present in a TE_{mn} configuration [4]. They can be written as:

$$H_z = \cos(\frac{m\pi x}{a})\ \cos(\frac{n\pi y}{b})\ e^{-j\beta z} \qquad E_z = 0$$

$$H_x = j\frac{\beta m\pi}{ak_c^2}\sin\left(\frac{m\pi x}{a}\right)\cos\left(\frac{n\pi y}{b}\right)e^{-j\beta z}$$

$$H_y = j\frac{\beta n\pi}{bk_c^2}\cos\left(\frac{m\pi x}{a}\right)\sin\left(\frac{n\pi y}{b}\right)e^{-j\beta z} \qquad (2.14)$$

$$E_x = \frac{kZ_0}{\beta}\, j\frac{\beta n\pi}{bk_c^2}\cos(\frac{m\pi}{a})\ \sin(\frac{n\pi y}{b})\ e^{-j\beta z}$$

$$E_y = -\frac{kZ_0}{\beta}\, j\frac{\beta m\pi}{ak_c^2}\sin(\frac{m\pi x}{a})\ \cos(\frac{n\pi y}{b})\ e^{-j\beta z}$$

The cutoff wave number (k_c^2) and propagation phase constant (β) are related by the following equations.

$$k_c^2 = \left(\frac{m\pi}{a}\right)^2 + \left(\frac{n\pi}{b}\right)^2 \tag{2.15}$$

$$\beta^2 = k^2 - k_c^2 \tag{2.16}$$

The lowest frequency which can be supported by a waveguide is known as the cutoff frequency and the dominant mode is the mode with the lowest cutoff frequency. For TE configuration, if a>b then the dominant mode is represented as TE_{10}. The cutoff frequency depends on the properties of the dielectric material filled inside the guide and also the mode number. It can be expressed as:

$$f_{cutoff} = \frac{k_C}{2\pi\sqrt{\mu\varepsilon}} = \frac{1}{2\pi\sqrt{\mu\varepsilon}}\sqrt{\left(\frac{m\pi}{a}^2\right) + \left(\frac{n\pi}{b}^2\right)} \tag{2.17}$$

$$\lambda_c = \frac{2ab}{(m^2b^2 + n^2a^2)^{1/2}} \tag{2.18}$$

where λ_c corresponds to the cutoff wavelength of the waveguide, 'a' is the width and 'b' is the height of the rectangular waveguide. For the dominant mode the cutoff frequency can be calculated by using the below equation:

$$f_{cutoff,TE_{10}} = \frac{1}{2\pi a\sqrt{\mu\varepsilon}} \tag{2.19}$$

where a is the width of the rectangular waveguide.

b. TM Modes

For the transverse magnetic (TM) mode the magnetic field component along the direction of propagation (H_z) doesn't exist. The other field components can be written as following:

$$H_z = 0$$

$$E_z = \sin\left(\frac{m\pi x}{a}\right) \sin\left(\frac{n\pi y}{b}\right) e^{-j\beta z}$$

$$H_x = -E_y / Z_e \quad , \quad H_y = E_x / Z_e$$

Where $Z_e = \frac{\beta Z_0}{k}$ (2.20)

$$E_x = -j\frac{\beta m\pi}{ak_c^2}\cos\left(\frac{m\pi x}{a}\right) \sin\left(\frac{n\pi y}{b}\right) e^{-j\beta z}$$

$$E_y = -j\frac{\beta n\pi}{bk_c^2}\sin(\frac{m\pi}{a}) \cos(\frac{n\pi y}{b}) e^{-j\beta z}$$

The wave-number and cutoff frequency calculation are similar to the TE mode. They are as follows:

$$k_c^2 = (\frac{m\pi}{a})^2 + (\frac{n\pi}{b})^2$$

$$\beta^2 = k^2 - k_c^2 \quad ; \quad \lambda_C = \frac{2ab}{(m^2b^2 + n^2a^2)^{1/2}}$$ (2.21)

It can be seen that the cutoff frequency of the dominant mode, i.e. TE_{10} mode doesn't depend on the height 'b' of the waveguide. So by decreasing the height to some extent won't have any effect on the performance. This gives rise to the discovery of SIW technology.

2.4.2 Substrate integrated Waveguide Filter

The substrate integrated waveguide technology was first introduced by *Ke Wu et al.* [5] in the year 2003, as a new concept for high-frequency integration circuits. SIW structure is based on a planar dielectric substrate with two parallel arrays of metallic vias connecting the top and bottom layer of the substrate [6]. As shown in Figure 2.7 the top and bottom metallic layers of the substrate are connected by the two walls of via-fence. SIW technology

is more popular over the classical waveguide technology due to the features like low-cost, mass-producible, high-Q factor [6], low-loss [5] and simple-structure.

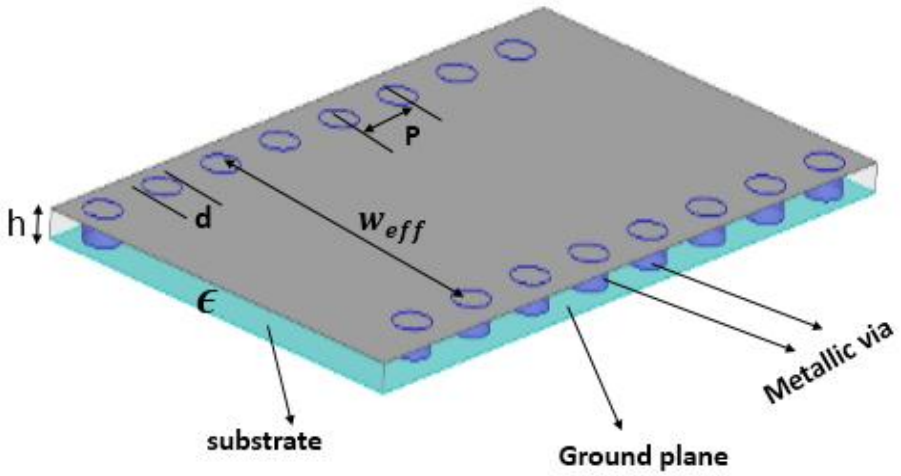

Figure 2.7 structure of Substrate Integrated Waveguide

From the Figure 2.7, the parameters of the SIW filter can be stated as:

h: Height of the Substrate

$\boldsymbol{\epsilon}$: Dielectric constant of the substrate

$\boldsymbol{W_{eff}}$: Effective width of the SIW

d: Diameter of the metallic via

P: distance between two consecutive vias

There are some basic rules and constraints involved with the calculation of the above parameters. Modelling, wave mechanisms, leakage characteristics and performance analysis are described in the literatures [12-14]. The basic design of a SIW filter includes the width calculation which depends on the cutoff frequency of the SIW. The calculation of effective width (w), via diameter (d) and gap between the two consecutive vias (p) are described in [5-6]. From [12], it can be observed that the modes present in the SIW are different from the modes which exist in a rectangular waveguide. The first step for designing any bandpass filter is to calculate the width of the waveguide according to the cutoff frequency.

(i) Effective width of the SIW

For the dominant mode of operation, the cutoff frequency of the waveguide depends only on the width of the guide. Therefore the height can be chosen as low as possible for designing the SIW. The relation between the width and cutoff frequency for TE_{10} mode is presented in [6, 7]:

$$f_{10} = \frac{c}{2w\sqrt{\varepsilon_r \mu_r}} \tag{2.22}$$

where ε_r and μ_r are the electric permittivity and magnetic permeability of the substrate.

Where w is the width of the SIW. The effective width and width are related by the following formula as in [12].

$$W_{eff} = w - 1.08*\left(\frac{d^2}{p}\right) - 0.1*\left(\frac{d^2}{w}\right) \tag{2.23}$$

where d: diameter of the via

However a more accurate formulation is given in [15], which includes via diameter'd' and via spacing (p) as written in Eq. (2.24).

$$f_{cTE_{10}} = \frac{c}{2\sqrt{\varepsilon_r}}\left(w - \frac{d^2}{0.95*p}\right) \tag{2.24}$$

The width calculation analysis is mostly done for the TE_{mo} modes because TE_{mn} modes doesn't exist in the SIW. That's discussed in the next session where supported modes for SIW are given.

(ii) Modes supported in SIW

Though the SIW structures are having similar behavior as conventional rectangular waveguides but the difference is still noticeable. First, the SIW is a guided-wave periodic structure which may lead to EBG (Electromagnetic band-gap) behavior. Secondly, due to presence of space between two consecutive vias the leakage losses are unavoidable. Therefore, the modes exist in SIW are kind of different from modes present in RWG. As given in [12], the numerical methods were applied to calculate surface current distribution in a SIW, where *TM* modes couldn't be extracted. So *TM* modes aren't present in the SIW.

Despite this TE_{mn} modes (where m and n both nonzero) aren't present due to the discontinuity in the regular waveguide structure. The surface current distribution is given in Figure 2.8. The only modes which exist in SIW structure are TE_{m0} modes, for instance $TE_{10}, TE_{20}, TE_{30}$ etc.

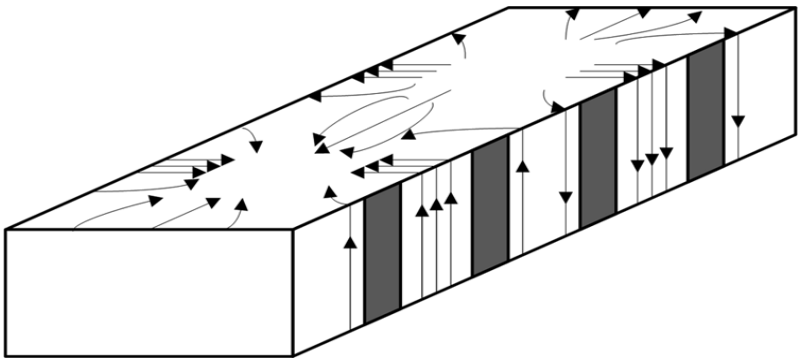

Figure 2.8: Surface current distribution [12]

(iii) Feeding mechanism

Feeding to a SIW plays a vital role in the design of the SIW filters. Since the SIW components like isolators, couplers, filters, etc. are needed to be integrated on the same PCB with other components, so planar transitions or feeding techniques are developed. Some of the most popular and efficient planar feeding techniques are microstrip line (MSL) feed, tapered feeding [16], tapered-via feeding [8] and Coplanar waveguide(CPW) feeding [9] . The E-field profiles for MSL and waveguide are shown in Figure 2.9, from which it can be observed that they share almost the same field-profile. Therefore using a microstrip line to excite the waveguide structure is quite possible since they have profiles oriented in the same direction. That's how these planar techniques are developed. Tapered feeding is a type of feeding in which the microstrip line is tapered out to provide impedance matching between the planar MSL and SIW as shown in Figure 2.9 (c). In this case the tapered-out line is able to match the impedance, but still there are some reflection losses due to the sudden transition from MSL to waveguide. A new technique is proposed in [8] to reduce these losses by providing a tapered-via feeding. In tapered-via feeding as shown in Figure 2.9(d), extra two vias are used in between the transition to make the transition smoother. In tapered and tapered-via feeding, the thickness of the substrate is reduced to provide impedance matching, which leads to the minimization of conductor loss but it also gives rise to an

increase in radiation loss in the MSL. That is the reason, these feeding techniques are not preferable for mm-wave frequency range. Hence, CPW-SIW feeding is used for mm-wave applications.

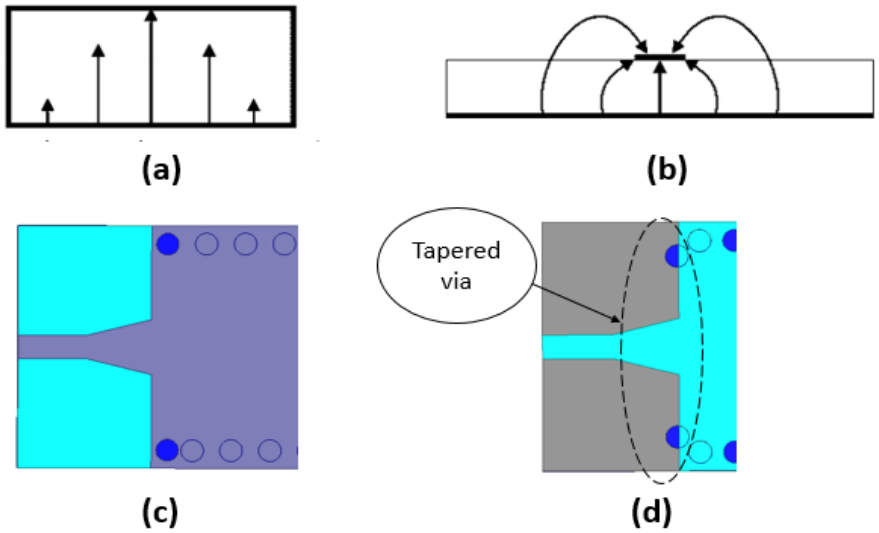

Figure 2.9: (a) E-field vector representation in a waveguide (b) E-field vector representation in a microstrip line [16] (c) Tapered feeding (d) Tapered-via feeding

In [17] a coplanar waveguide excitation is used to provide feeding to a SIW structure as shown in Figure 2.10. In this type of excitation, the feed line is placed as an inserted stub and it requires only single plane for the feeding. Though the increase in height of the substrate leads to losses in the tapered feeding techniques, but CPW isn't sensitive to the thickness of the dielectric material. Therefore it provides better performance in very high frequencies like mm-wave frequencies. However, CPW-SIW has got a lower bandwidth as compared to the normal microstrip line feed. That's the reason UWB applications don't use CPW feeding. Still there is provision for modified CPW feeding techniques for bandwidth improvement.

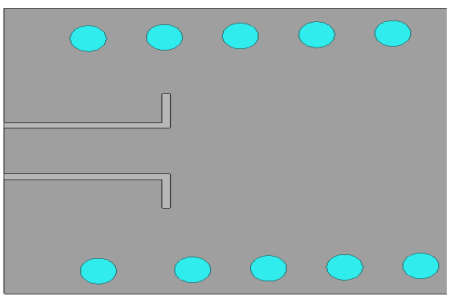

Figure 2.10: CPW to SIW transition

(iv) Losses present in SIW

There are basically three types of losses present in a substrate integrated waveguide. Which are:

- Conductor losses
- Dielectric or substrate loss
- Radiation or leakage loss

Conductor losses are present due to the finite electric conductivity of the top and bottom metal layers. Dielectric or substrate loss is also a type of conducting loss which is due to the loss tangent of the dielectric material used as a substrate. At high frequencies i.e. mostly at mm-wave applications the proper choice of substrate material plays an important role, because when the frequency increases the major contribution to losses is provided by dielectric material. As given in [13], due to presence of gaps between the metallic posts, there is a leaky wave propagates in the SIW which is responsible for the leakage or radiation losses. The radiation losses can be calculated using the relation in Eq. (2.25) in [3].

$$\text{Radiation loss} = \left(1-\left|S_{11}\right|^2-\left|S_{21}\right|^2\right) \tag{2.25}$$

where S_{11} and S_{21} are the reflection and transmission coefficients or the scattering parameters.

Now since these losses are present which can't be avoided, but the design considerations may be applied to minimize these losses. So comes the design rules into picture which is clearly stated in [12-14]. The formulations consider:

- Proper choice of post diameter.
- Proper choice of via spacing in terms of via diameter.

The formulations were developed using a large amount of simulation and experimental data. Choosing the via diameter 'd' depends on the guided wavelength 'λ_g' as:

$$d < \frac{\lambda_g}{5} \tag{2.26}$$

Via spacing 'p' should be, such that:

$$p \leq 2d \tag{2.27}$$

These two rules are not mandatory but sufficient, since choosing a specific via diameter is not always possible due to the presence of fabrication constraints.

2.4.3 Half-mode SIW filters

Half-mode SIW (HMSIW), yet another concept in integrated waveguide technology which was first proposed by *wei hong et al.* [18]. HMSIW is an integrated guided-wave structure which is half in size as compared to conventional SIW but gives almost the same performance as shown in Figure 2.11. This kind of structure is possible because of the magnetic wall behavior shown by the symmetric plane along the direction of propagation. So, even the size of SIW is cut to half, still the field behavior is unchanged.

Two models of HMSIW are described in [19]. First, to calculate the field distributions inside a HMSIW and another to obtain an approximate formula for calculation of the effective width of HMSIW. Numerical analysis was used in [19] to show the different possible field profiles in HMSIW.

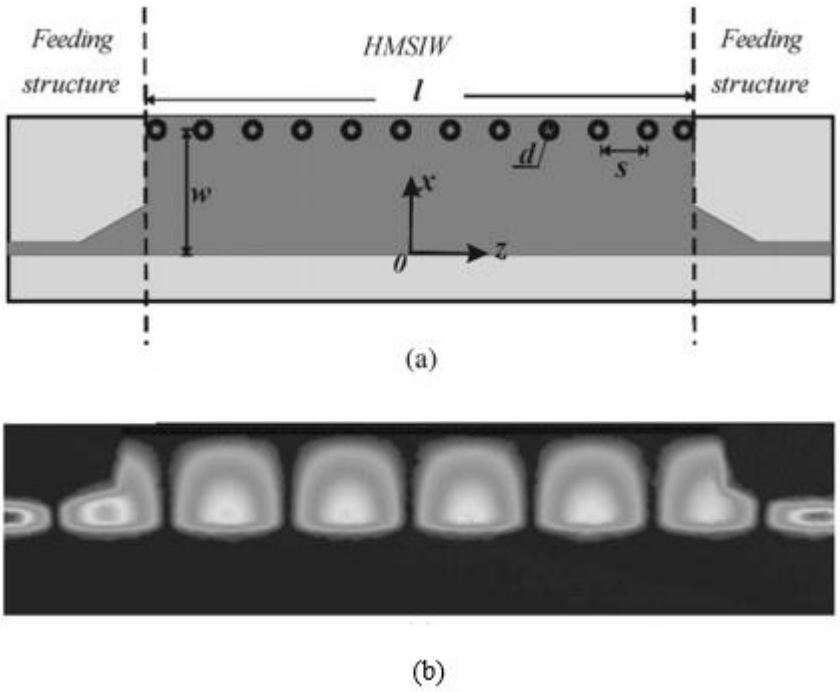

Figure 2.11: (a) Structure of HMSIW (b) Field profile in HMSIW [19]

(i) Modes present in HMSIW

The width to height ratio is large in HMSIW, so it supports only quasi $\boldsymbol{TE_{m*(0.5),0}}$ modes , where m = 1, 3, 5, 7….. as characterized in [19]. This is similar to half of the dominant mode in SIW i.e. TE_{10} . In the Figure 2.11 (b), the field pattern of the dominant mode in HMSIW is presented. For instance the modes possible in HMSIW would be $TE_{0.5,0}$, $TE_{1.5,0}$, $TE_{2.5,0}$ etc…

(ii) Effective width calculation of HMSIW

The effective width calculation for the HMSIW is similar to the width calculation carried out in SIW. Effective width can be calculated using Eq. (2.28) in [19]. The effective width of HMSIW is half the width of SIW.

$$W'_{eff,HMSIW} = \frac{W_{eff,SIW}}{2} \tag{2.28}$$

where $W'_{eff,HMSIW}$ = effective width of the HMSIW

$W_{eff,SIW}$ = effective width of the SIW

Effective width of the SIW can be written as below:

$$W_{eff,SIW} = 2w - 1.08\frac{d^2}{p} - 0.1\left(\frac{d^2}{2w}\right) \tag{2.29}$$

where 2w = actual width of the rectangular waveguide

P= pitch or via spacing

d = diameter of the via

Due to the fringing effect in the microstrip line the actual width of the HMSIW becomes:

$$W'_{eff,HMSIW} = W_{effHMSIW} + \triangle w \tag{2.30}$$

This additional width ‘ $\triangle w$ ’ can be calculated using the Eq. (2.31).

$$\frac{\Delta w}{h} = \left(0.05 + \frac{0.3}{\varepsilon_r}\right) * \ln\left(0.79 * \frac{W'^2_{effHMSIW}}{h^3} + \frac{104W'_{effHMSIW} - 261}{h^2} + \frac{38}{h} + 2.77\right) \tag{2.31}$$

Effective width and cutoff frequency of a HMSIW are related as follows:

$$f_{cTE0.5,0} = \frac{c}{4W_{eff,HMSIW}\sqrt{\varepsilon_r}} \tag{2.32}$$

The losses in HMSIW are either at the same level or even lower than the losses present in SIW when identical materials are used and arrangement of vias are similar. A more detailed and extensive use of HMSIW technology for bandpass filter design has been given in chapter 4.

2.5 Summary

In this chapter a brief study about microwave filters, their use and design methodology has been discussed. Along with this the basics of SIW bandpass filters and their relationship with the rectangular waveguides are also studied. Different types of feeding mechanisms and calculation of basic parameters involved in the design of SIW filters are described with the use of various formulae and figures. Basic features of Half-mode SIW and its use to make compact filter designs are also briefed. These fundamentals of filter design is used in the chapter 3 to design SIW filters for different microwave bands.

Chapter 3

Design and analysis of a class of compact SIW bandpass filters

3.1 Introduction

In this chapter a class of compact and high performance SIW bandpass filters are proposed using tapered-via transition and a simple EBG structure. The proposed filters are designed for Ku band (12-18GHz) and S-band (2-4GHz) of the microwave frequencies. The filters were designed and simulated using High frequency Structural Simulator (HFSS). The proposed filters are designed and simulated on a low cost FR4 substrate by the HFSS v14. The S-band filter is fabricated using FR4 substrate. The improvement in results are also described and compared with similar designs reported in the literature.

3.2 SIW filter Design process

Design of the basic model includes calculation of width, via diameter and via spacing of the SIW filter. However, there are other calculations due to the use of tapered-via and u-slotted EBG structure. The basic theory for designing a SIW bandpass filter is discussed in the following section.

3.2.1 Theory

A basic structure of an SIW consists of the top and bottom metal planes of a substrate and two parallel arrays of via holes (also known as via fence) integrated in the substrate as shown in Figure 3.1.The width of the SIW filter is calculated by using Eq. (3.1) corresponding to the lower cutoff frequency 'f_{cutoff}' of the dominant mode (TE_{10}) [10].

$$f_{cutoff} = \frac{c}{2w\sqrt{\epsilon_r}} \tag{3.1}$$

where design parameter 'w' is the width of SIW, 'ϵ_r' is the dielectric permittivity of the substrate used for the construction of SIW structure and 'c' is the velocity of light in free space.

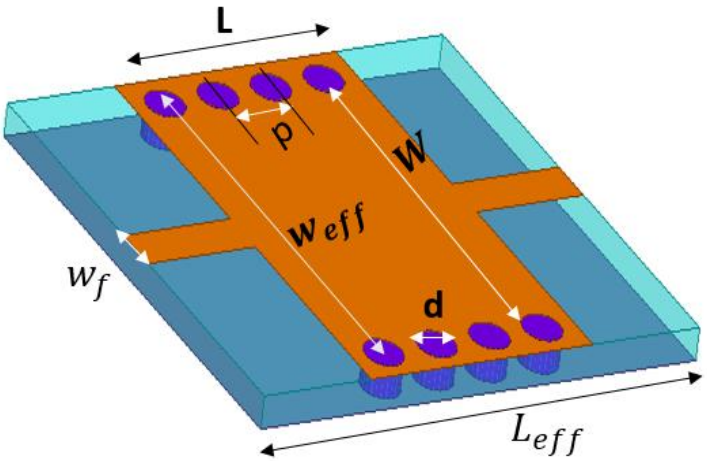

Figure 3.1: Basic model of SIW filter

In the Figure 3.1 the different geometrical parameters are defined as:

W_f = width of the microstrip feed line

d = diameter of the via

P= via spacing

L = length of the SIW

W= width of the SIW

w_{eff}= effective width of SIW

Increase in via spacing 'p' between the consecutive posts lead to increase in radiation or leakage loss of the SIW structure and also diameter 'd' has some constraints as described in chapter 2. Hence, the selection of proper location of the vias and diameter of the holes in the SIW structure are critical design parameters. The dimensions of array of vias are optimistically calculated by using Eq. (3.2) and Eq. (3.3).

$$d < \frac{\lambda_g}{5} \tag{3.2}$$

$$p \leq 2d \tag{3.3}$$

where 'λ_g' is the guided wavelength and is determined by using Eq. (3.4).

$$\lambda_g = \frac{\lambda_{ms}}{\sqrt{\epsilon_{r_{eff}}}} \tag{3.4}$$

Here, 'λ_{ms}' is the wavelength of the microstrip feed line corresponding to centre frequency 'f_c' of the bandpass filter and '$\epsilon_{r_{eff}}$' is the effective dielectric constant. 'f_c' is calculated using Eq. (3.5).

$$f_c = \frac{f_l + f_h}{2} \tag{3.5}$$

where f_l and f_h are the lower and higher cut-off frequencies in the pass band of the filter.The width of the waveguide port 'w' is calculated by using Eq. (3.6), described in [7].

$$w = \frac{c}{2\, f_{cutoff} \sqrt{\epsilon_r}} \tag{3.6}$$

3.2.2 Tapered via transition

Tapered via or modified taper is used for MSL to SIW transition. A wideband transition from microstrip line to SIW structure, consists of a microstrip line along two extra vias are used as a feed-line to the SIW which is proposed in [8] and is shown in Figure 3.2.

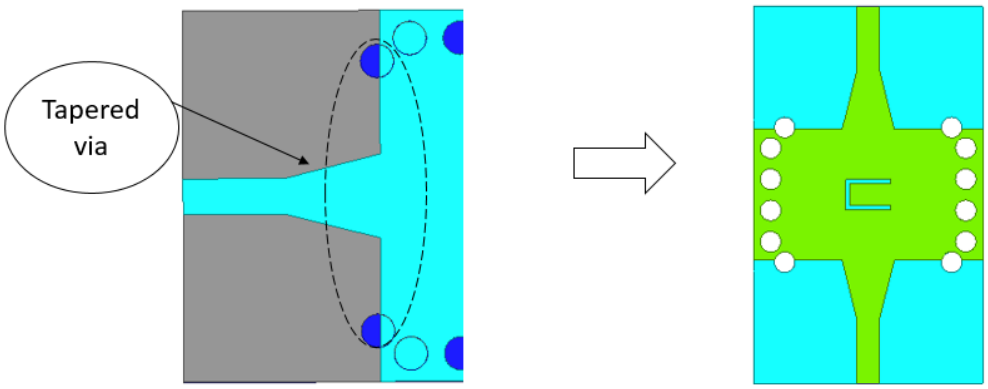

Figure 3.2: Tapered via transition

The feedline i.e. transition from microstrip line (MSL) having an impedance of 50 Ohms to SIW having impedance less than 50 Ohm is tapered out in order to get the lowest reflection loss in the passband. Two metallic vias are added at the transition of tapered microstrip line to SIW structure to achieve a wide band with better isolation. The physical dimensions of taper, i.e. length 'l_{tap}' and width 'w_{tap}' are calculated using the analytical expressions given in [8]. The length of the taper is calculated by:

$$l_{tap} = \frac{\lambda_g}{4} \tag{3.7}$$

The width of the taper w_{tap} is calculated as:

$$w_{tap} = w_f + 0.154*l \quad (3.8)$$

where w_f is the width of the microstrip feedline and l is the width of the SIW filter.

3.2.3 Design of EBG structure using 'U' slot

As given in [9-11] the 'U' slot behaves as an EBG (electromagnetic band gap) by creating a stopband in the transmission range of the SIW filter. In the basic design as shown in Figure 3.3 one U-slot is made at the Centre for creating a stopband at the upper stop-band of the filter.

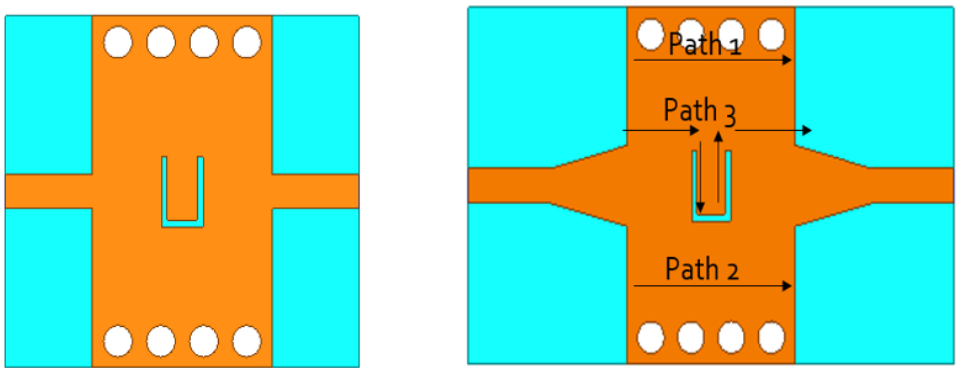

Figure 3.3 (a) U-slot design (b) Wave travelling mechanism

Figure 3.3(b) shows a 180^o delay which is responsible for the transmission zero in the upper stopband region of the filter, since in the path -3 a phase difference is created between the incoming and the outgoing waves. That's how 'U' slot introduces a stopband zero and as a result the stopband behavior improves. The length or height of the slot is crucial parameter for calculating the stopband zero frequency since they are related inversely as given in the Eq. (3.9).

$$f_z = \frac{c}{4\, l_s \sqrt{\epsilon_r}} \quad (3.9)$$

where l_s = length of U slot

f_z = frequency at which the transmission zero has to be introduced

3.3 Design of a SIW band-pass filter for Ku band

In this section a SIW bandpass filter is proposed by using tapered via and multiple U-slots for having applications in Ku band (12-18GHz) region. The filter is designed in the HFSS software using low-cost and easily available FR4 substrate having dielectric constant (ϵ_r=4.4), dielectric loss tangent 0.02 and height 0.5mm.

3.3.1 Design flow

The flow or structure of the designed filters are shown in Figure 3.4. The Figure shows how the basic structure is modified along the way to get the final design. All the filters were designed for Ku band of operations only.

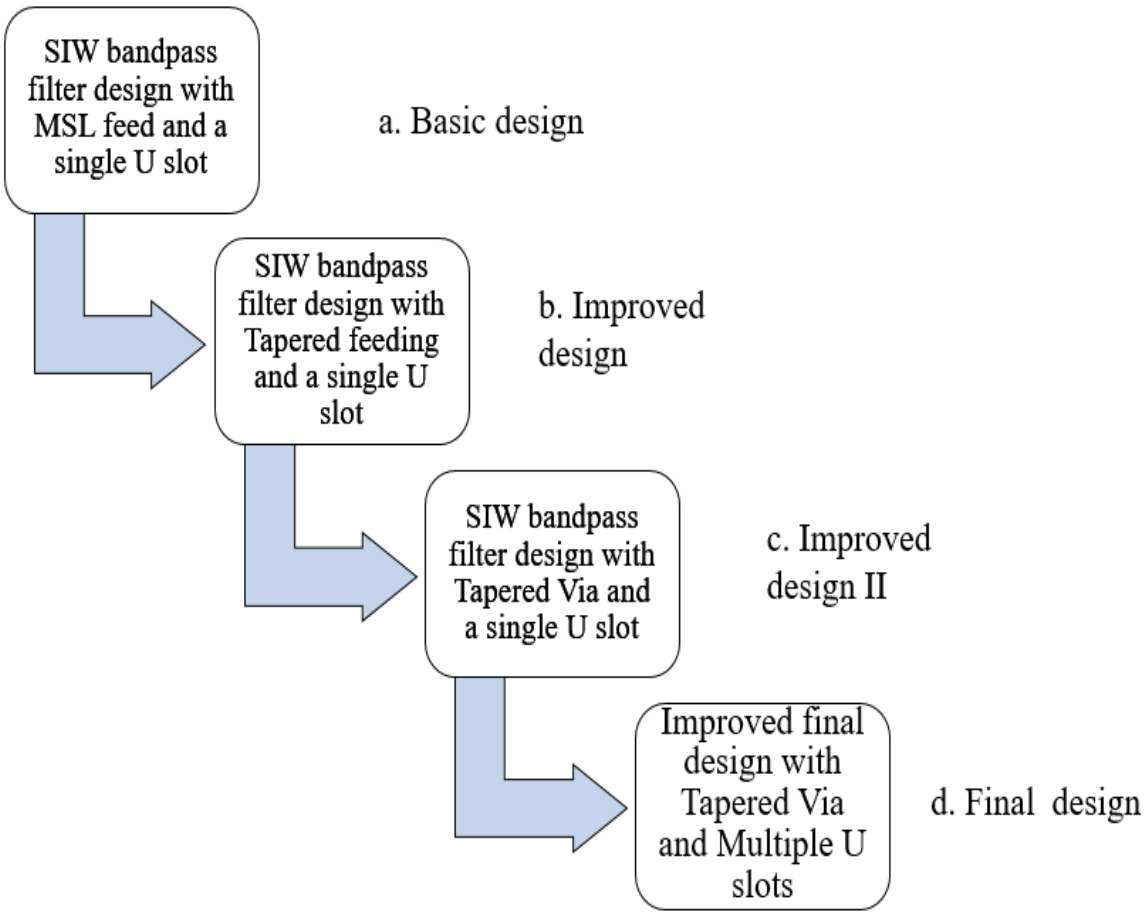

Figure 3.4: Ku band filter design flow

3.3.2 Geometry and calculation of the dimensions

The dimensions for the filters are calculated using the Eq. (3.1) to (3.9) keeping in mind the following desired requirements, as they are designed to be operated in Ku band (12-18GHz). The design specifications can be summarized as follows:

- Cutoff frequency for Ku-band: 9.5GHz
- Center frequency of the passband: 14.5GHz
- Upper stopband zero frequency: 20GHz
- Proper choice of d and p.

The SIW filter proposed in [9] is used to make the basic design for Ku band. In basic design, due to the existence of a single 'U' shaped slot, the stopband loss is maximized as the 'U' slot leads to a transmission zero in the stopband. The basic design has less bandwidth and degraded performance due to impedance mismatching. With improved design, a tapered transition which provides a smooth transition from microstrip line to SIW structure is presented to enhance the return loss performance and bandwidth. Further, in improved design-II the modified version of improved design with two vias at the transition from MSL to SIW is proposed. Further, S_{11} performance is improved due to the presence of two extra vias. Eventually, in the final design, improved design-II is modified with the addition of four numbers of U-slots arranged symmetrically about two parallel rows as shown in Figure 3.5(d). The presence of multiple 'U' slots corresponds to the improvement in the stopband response. The structures showing top view and dimensions of the designed filters are shown in the Figure 3.5.

The SIW filters are designed using a double-sided copper clad FR4 (dielectric constant (ϵ_r) =4.4, thickness 0.5 mm, loss tangent 0.02 S/m) substrate due to its ease in availability & low-cost. The calculated parameters are fine-tuned later using parametric analysis and inbuilt optimizer present in HFSS v.14. The final design parameters of all the SIW filters are given in TABLE 3.1.

Table 3.1: Design dimensions of the Proposed SIW Filters

Design parameters (in mm)	**Basic Design**	**Improved Design**	**Improved Design II**	**Final Design**
L	5.621	5.621	5.621	5.621
w_{eff1}	11.12	--	--	--
w	7.58	7.58	7.58	7.58
w_{eff}	8.48	8.49	8.49	8.49
$w1$	9.90	9.90	9.90	9.90
p	1.35	1.35	1.35	1.35
d	0.90	0.90	0.9	0.9
l_{mf}	2.72	2.72	2.72	2.72
w_f	0.955	0.955	0.955	0.955
w_{eff2}	-	16.3	16.3	16.3
l_{tap}	-	2.58	2.58	2.58
w_{tap}	-	2.26	2.26	2.26
l_s	1.98	1.98	1.98	1.98
t_s	1.30	1.30	1.30	1.30
w_s	0.1887	0.1887	0.1887	0.1887
p_1	-	0.885	0.885	0.885
w_v	-	7.26	7.26	7.26
g	-	-	-	0.60
m	--	-	--	6.46
s_1	-	--	-	0.521

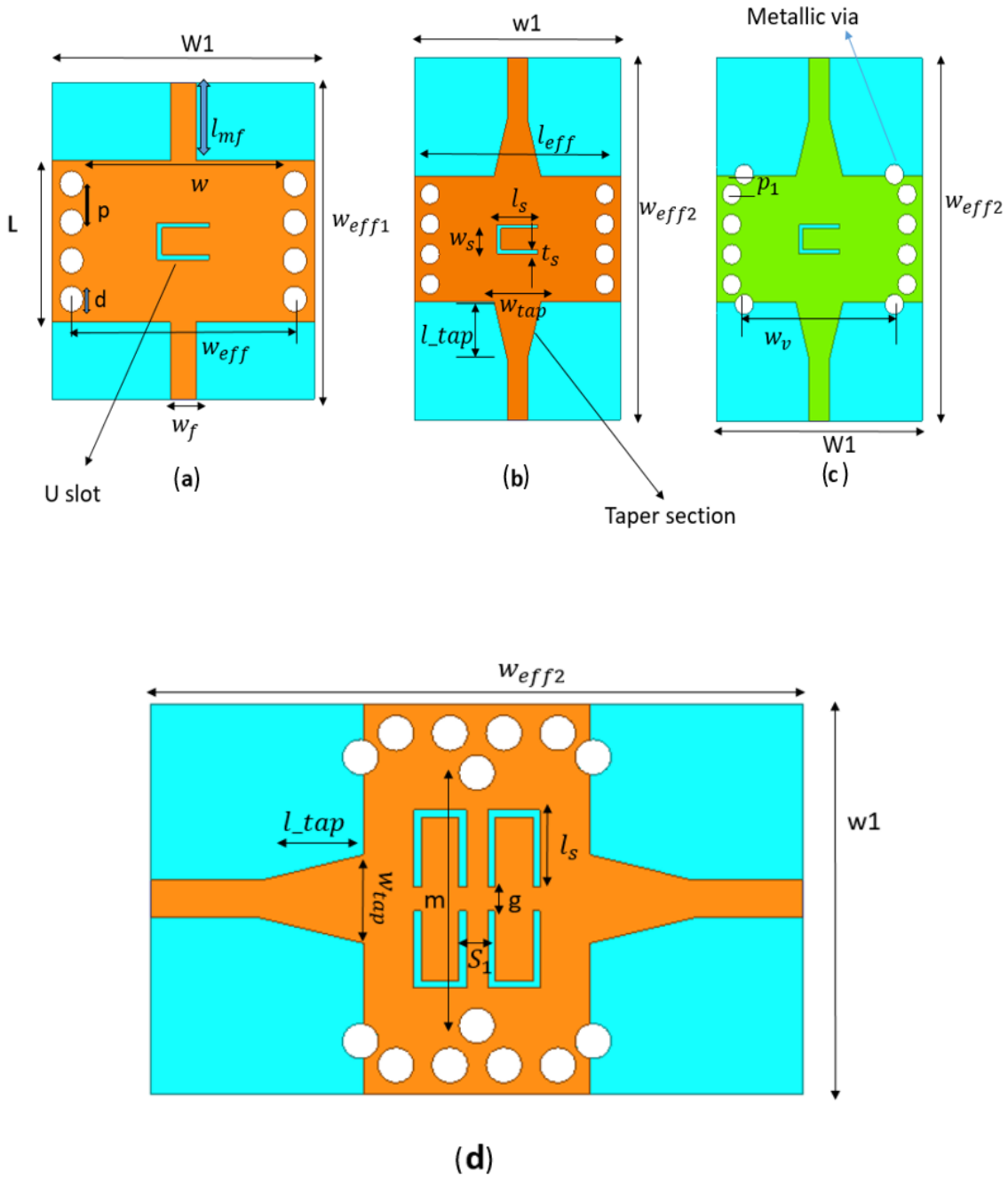

Figure 3.5: Structure of the designed SIW filters (a) Top view of the basic design (b) Top view of the Improved Design (c) Top view of the Improved Design II (d) Final design

3.3.3 Results and analysis

A detailed analysis of simulation results of the performance parameters like S_{11}, S_{21} , group delay and radiation loss of the filters presented in this section.

(i) S_{11} and S_{21} performance

The return loss performances are as shown in Figure 3.6. The results show that for the basic design, the passband is not wide enough to accommodate the Ku band frequencies as the S_{11} curve for a band of frequencies in the passband region go above the -10 dB reference level. This is normally due to the sudden transition in the impedance level of the microstrip feedline to the SIW structure. So, this problem is quite solved in improved design, by using a tapered transition between MSL and SIW structure. As the tapered transition provides a smooth continuity, the complete passpand (9.31 GHz - 17.22 GHz) is achieved in improved design. Later, in improved design-II, two metallic vias are introduced between tapered microstrip line and SIW structure for the smooth transition from the planar microstrip structure to waveguide structure with minimized reflection. This results in further improvement in the return loss of the filter as maximum S_{11} value attained is -44.1 dB. The final design provides a better S_{11} value of -53.143 dB at the frequency of 14.51 GHz due to the introduction of multiple 'U' slots as shown in Figure 3.8.

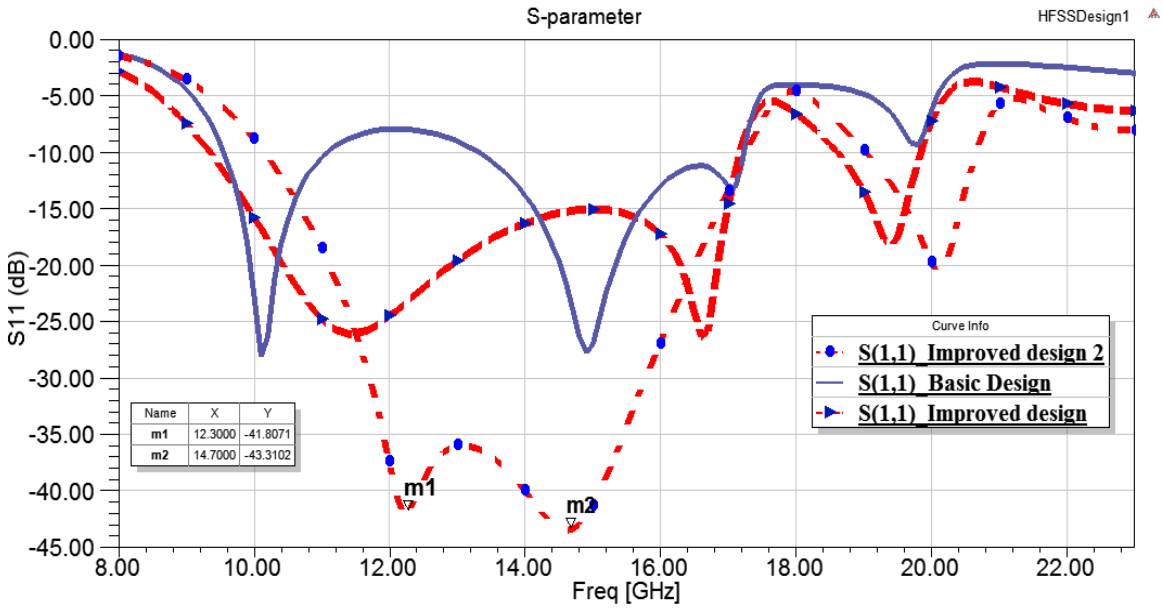

Figure 3.6: S_{11} performance of a, b and c (first three designs)

Insertion loss plots are as shown in Figure 3.7. The results show that the insertion loss stays below 1.9 dB in the pass band region for the first three designs. However, the stopband performance of these filters aren't good enough due to absence of a stopband zero. Finally, the stopband response of the final design is improved significantly as shown in Figure 3.8. This is attained by the introduction of multiple 'U' shaped slots arranged in two parallel arrays in the SIW structure which creates a transmission zero in the upper-stopband and hence the insertion loss attains its maximum value of 20.1 dB at a frequency of about 20 GHz.

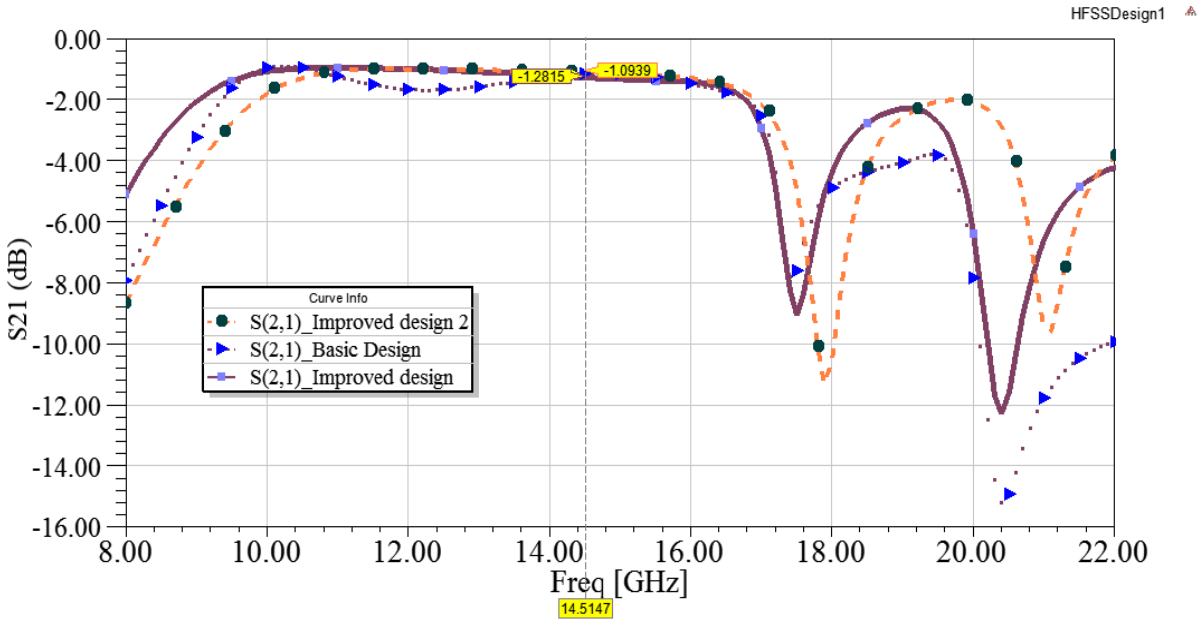

Figure 3.7: S_{21} performance of the a, b and c

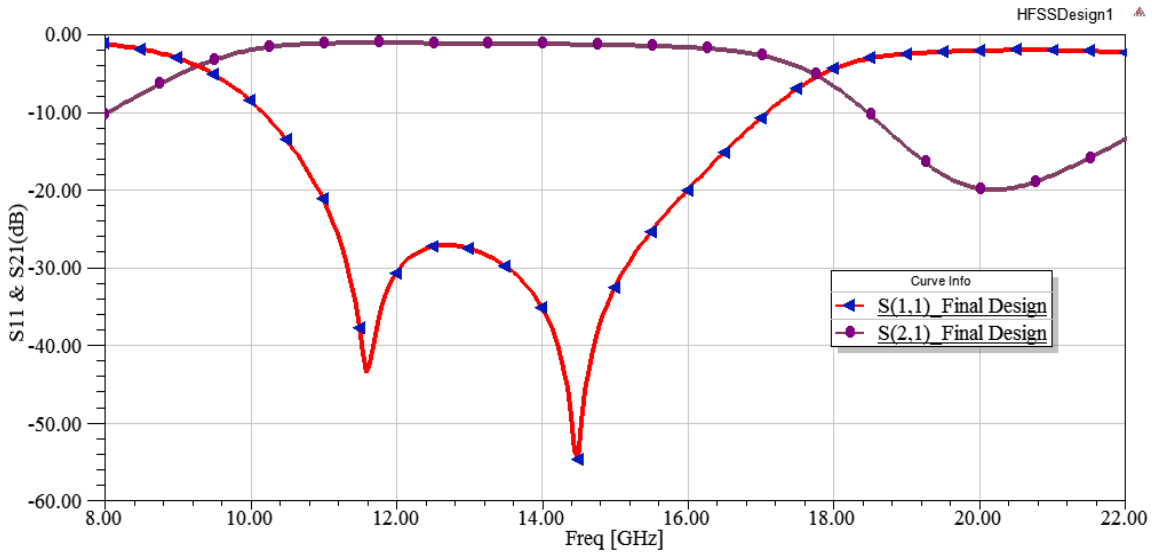

Figure 3.8: S_{21} and S_{11} curve of the Final design (d)

(ii) Group delay

Group delay is plotted against frequency. The group delay for the final proposed design comes out to be 0.242ns (maximum) and 0.161ns (min.) in the entire passband region of the filter as shown in Figure 3.9. This indicates that in the passband, the delay provided to all the frequencies are constant and same, which behavior is normally observed in linear systems.

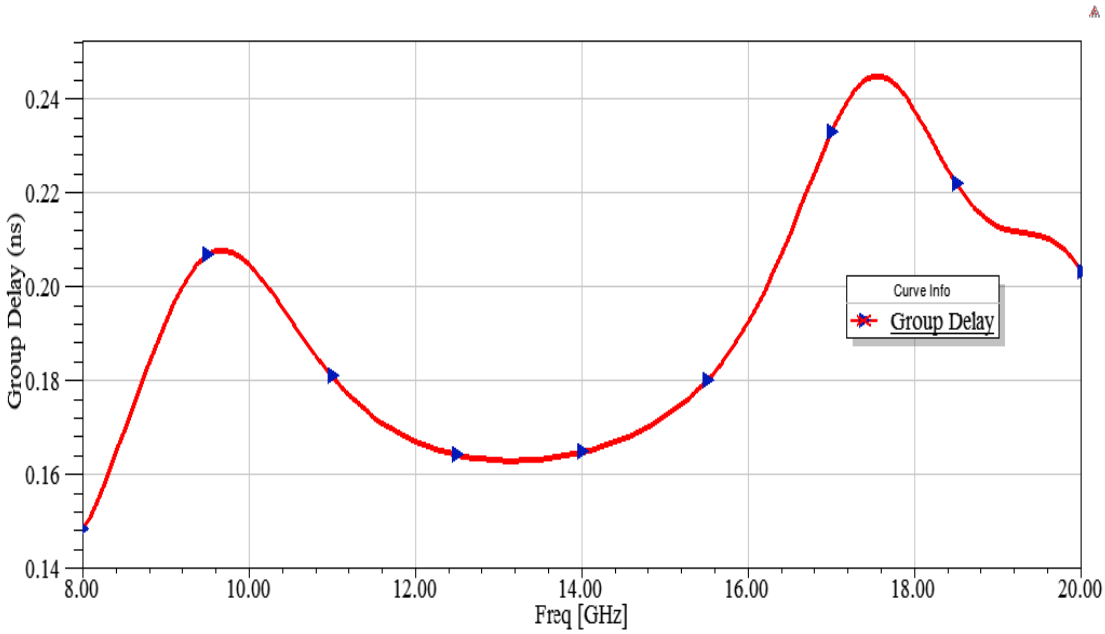

Figure 3.9: Group delay profile of the Final design

(iii) Radiation loss

Radiation loss is resulted due to the leaky wave and loss tangent (δ) of the substrate used in the design. It can be calculated by using ($1 - |S_{11}|^2 - |S_{21}|^2$) as given in chapter 2. The radiation loss is then plotted against frequency is shown in Figure 3.10. It shows that the radiation loss is below 20% in the passband of the proposed final design. This can be further reduced by using low-loss substrates like Roger RO4350, etc.

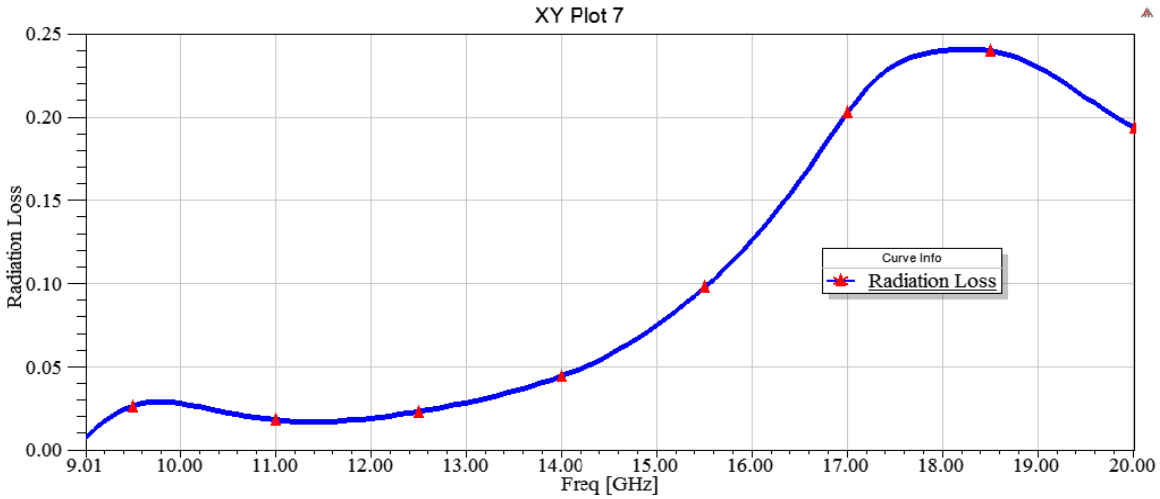

Figure 3.10: Radiation loss of the final design

3.3.4 Performance analysis

The simulation results obtained are summarized in the TABLE 3.2. From the table it's implied that, the final proposed design achieves the improved performance in terms of low reflection, the minimum value of group delay, better isolation and radiation loss. Hence, the proposed filter can be considered appropriate for the Ku-band applications. The simulated results of proposed final design are compared with the simulation results of existing SIW filters in the literature for Ku band applications, as presented in TABLE 3.3. The proposed SIW filter shows a decent amount of improvement in case of performance as compared to the SIW filters reported in literatures.

Table 3.2: Simulated performance parameters of the designed filters

Result Analysis	**Basic Design**	**Improved Design**	**Improved Design II**	**Final Design**
f_L *(GHz)*	9.55	9.30	10	10.19
f_H *(GHz)*	17.22	17.22	17.22	17.05
S_{11} *(in dB)*	< -8	<-10	<-10	<-10
S_{11} *(in dB) (Best case)*	-26	-25.74	-43	-54
S_{21} *(in dB)*	>-4.20	> -2.40	> -2.25	> -2.20

Table 3.3: Comparison of Performance among Proposed SIW Filter with other SIW Filters for Ku Band Applications

Design proposed by	Substrate	Insertion Loss (dB)	Return loss (dB)	3dB FBW (%)	Footprint (mm^2)	f_c (Center Freq.) (GHz)
[20]	KYOCE RA A493	1.41	>10	10	545	12.6
[21]	RO4350	1	>5	23	1915	15.75
Proposed final Design	FR4	1.13	>10	51	160	13.5

The proposed design possesses better stop-band characteristics due to the existence of multiple 'U' shaped slots. A part of this work has been published in [22]. The SIW structure introduces transmission zeros in the upper stopband region of the filter. The taper-via transition at the planar to SIW provides lower reflection which results in wide bandwidth of the filter. The overall size or footprint of the filter is 160 mm^2 which signifies its compactness. The proposed design possesses minimum return loss, better isolation, decent fractional bandwidth (FBW) of 51%. It is compact in size, low in cost and easier to fabricate than the other complex designs mentioned in the literature.

3.4 Design of a SIW band-pass filter for S-band

The S-band (2-4GHz) is a part of the EM spectrum for microwave applications. This band is used by weather forecasting radars, ship-surface radars and communication satellites. Since the applications in this band are broad and needs equipment's to work in strict environments, so a SIW bandpass filter is designed for this band which is capable of high power handling and compact in size as compared to a conventional waveguide. The proposed filter has been fabricated using a low-cost substrate FR4 (loss tangent=0.02, ϵ_r= 4.4 and thickness=1.6mm).

3.4.1 Design geometry

Design flow consists of two designs. First, the basic design in which four u-slots are used to get a stopband zero and two transmission poles in the passband. However the passband

return loss can be further minimized by making another pair of U-slot in the center of the structure arranged back to back as shown in Figure 3.11 (b). The calculation of these parameters are calculated according to the center frequency of 3GHz and cutoff frequency 1.5GHz.

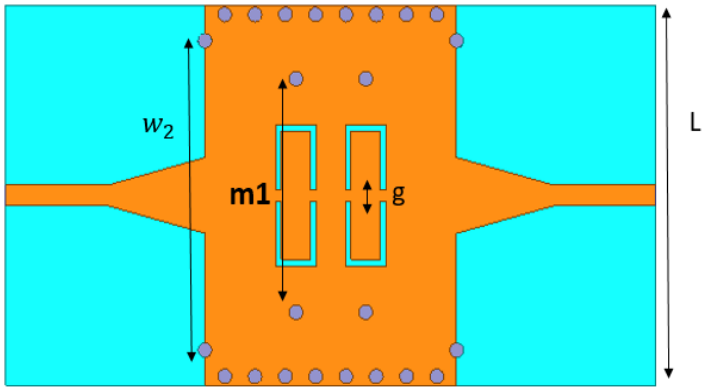

(a)

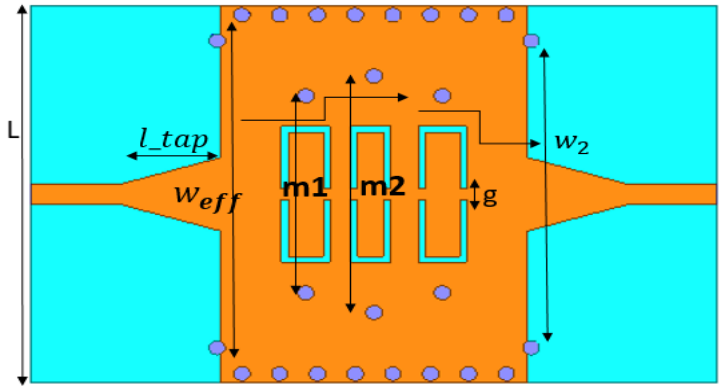

(b)

Figure 3.11 (a) Basic design of the S-band filter (b) final design

3.4.2 Calculation of the dimensions

The dimensions like width of the SIW filter, height of the U-slot , length of taper and width of the taper are calculated by the same process as it was given in the previous section, where these dimensions were calculated for Ku-band filter. However some dimensions like ‘m2’, gap ‘g’ and via width ‘w2’, via diameter ‘d’ and via spacing ‘p’ are calculated using parametric analysis and inbuilt optimizer to attain the best parametric values. Some of the important dimensions are given in the Table 3.4. The distance between the second set of vias around the U-slots i.e. ‘m2’ is chosen as:

m2= 1.3*(m1) (3.10)

By introducing this structure in the final design, a better bandwidth is achieved and reflections are also reduced in the passband.

Table 3.4: Dimensions of the designed structures

Design parameters (in mm)	Basic Design	Final Design
L	53	53
$w2$	42.5	42.5
p	3.5	3.5
d	2	2
l_{tap}	14	12.1
w_{tap}	10.4	10.4
g	1.5	1.5
m1	28	28
m2	--	37

3.4.3 Results and analysis

Simulations are carried out using HFSS V.14 and results obtained are discussed in the following sections.

(i) S-parameter curves

The return loss and insertion loss curves are as shown in Figure 3.12 and Figure 3.13 respectively. From this, it's clearly observed that filter provides the passband of 1GHz (2.5-3.5GHz) and stopband for frequency band greater than 4GHz. In the basic design, two resonances present in the passband i.e. at 2.9 GHz and 3.4 GHz with return loss of 29dB and 26dB respectively. However in the final design, due to introduction of a pair of U-slots, the resonance becomes better and the return loss is reduced to a value of 64.4dB at a frequency of 3.22GHz in the passband. For final design, the S21 value is also improved from -20dB to -34.44dB in the stopband of the filter.

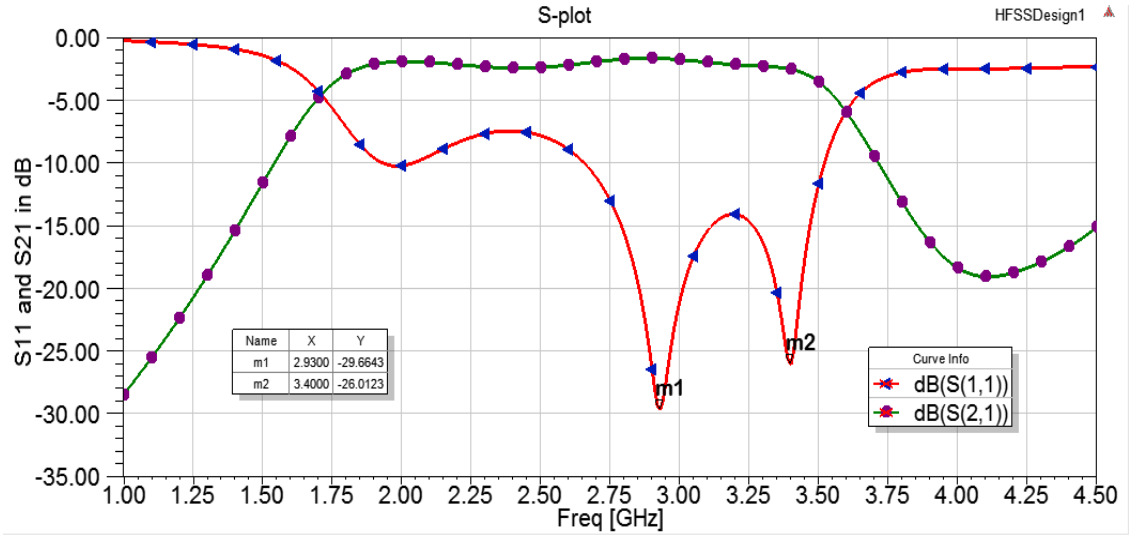

Figure 3.12 S-parameter curve of the basic design

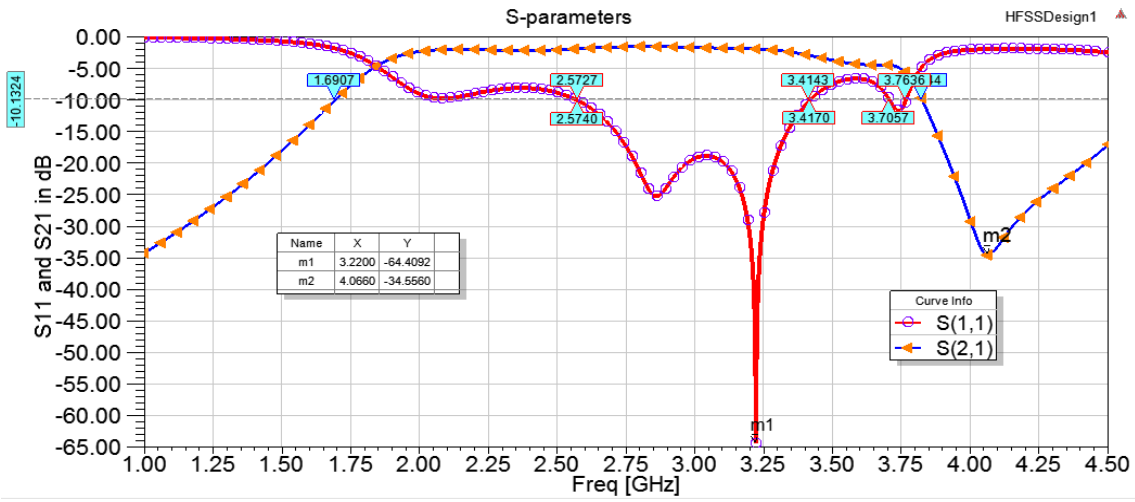

Figure 3.13 S-parameter curve of the final design

In the Figure 3.14, a comparison between the two designs in terms of scattering-parameters are presented. The bandwidth of the final design is comes out to be around 1GHz or FBW of 30% as can be seen from Figure 3.13. Insertion loss in the passband is around 2dB, which can be reduced by using high quality and low-loss substrate materials like Rogers RT/Duroid 5880.

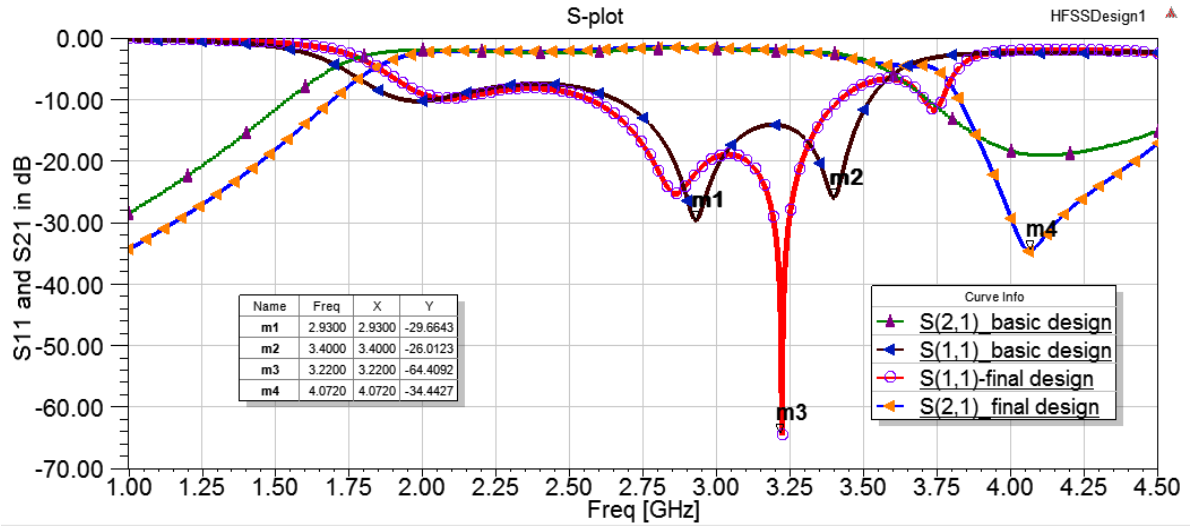

Figure 3.14: S-parameter curves for the designed S-band filters

(ii) Group delay

The group delay for both the designs are having similar pattern and almost same in the passband of the filter i.e. a maximum value of 2ns (Nano sec) and a minimum of 0.9ns in the passband. The curve almost shows a constant value in the entire passband as shown in Figure 3.15 which shows linearity of the filtering networks.

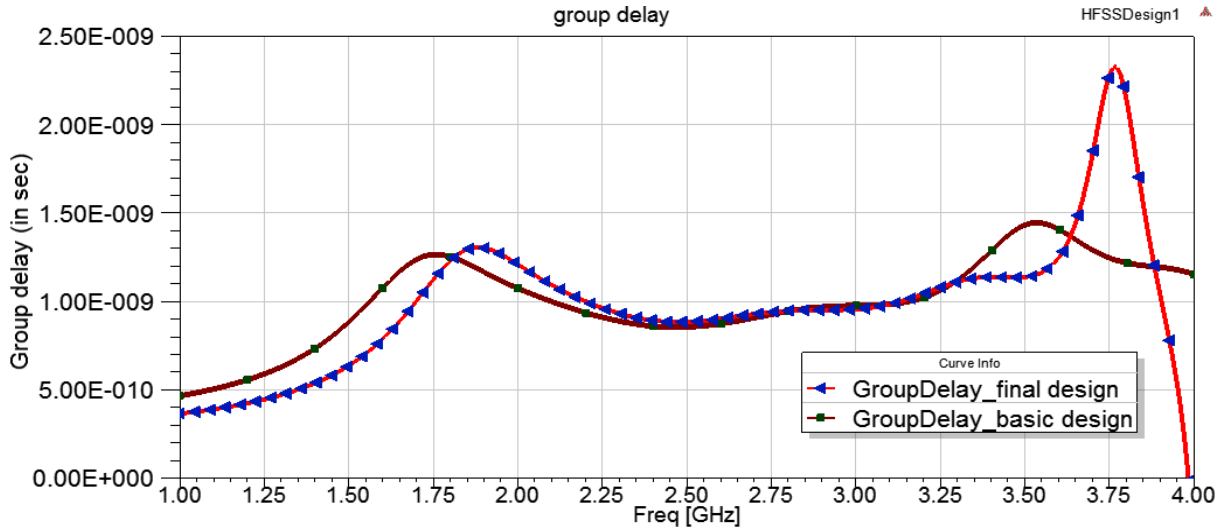

Figure 3.15: Group delay of the S-band filters

3.5 Fabrication

The final design has been fabricated using a low-cost substrate FR4 (loss tangent=0.02, ϵ_r= 4.4 and thickness=1.6mm) as shown in Figure 3.16. The return loss is measured using Vector Network analyzer (VNA) E5071C. The measured results are matching closely with the simulated as shown in the Figure 3.17.

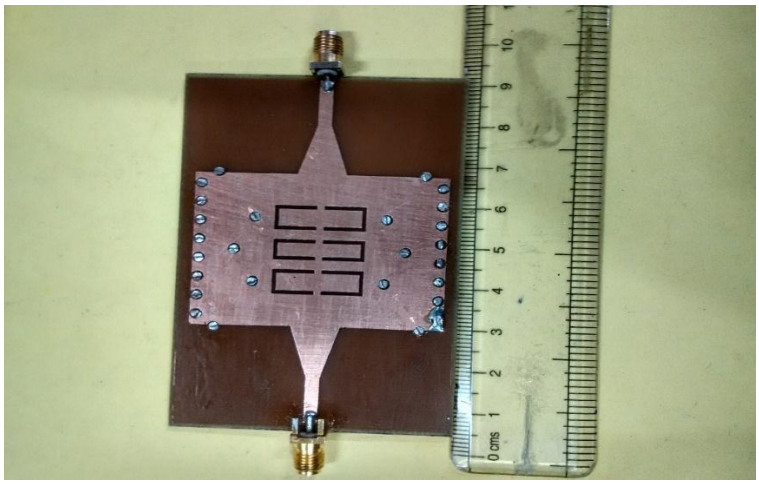

Figure 3.16: Fabricated S-band SIW filter

However, the slight mismatch between the measured and the simulated one may be due to the lossy nature of the substrate & the connecting cables used for the measurement.

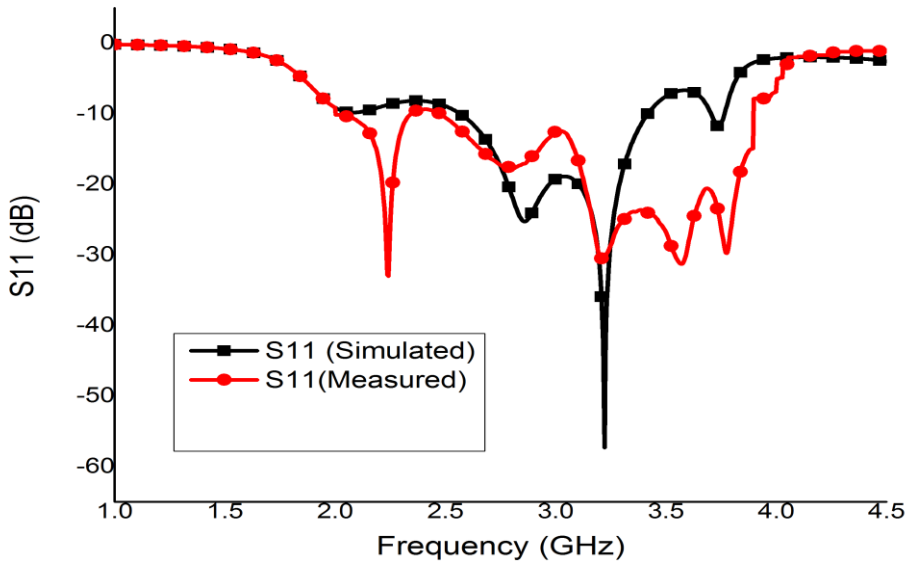

Figure 3.17: S_{11} curves for the S-band filters

3.6 Summary

This chapter summarizes into the design of two compact SIW bandpass filters for Ku-band and S-band applications using simple EBG structures and tapered-via feeding. The simulation results obtained are well described using Scattering plots, group delay and radiation loss curves. A compact and improved Ku band bandpass filter with a smooth planar microstrip to SIW transition having multiple 'U'-slots is proposed in this chapter. The performance is also compared with other similar filters in the literature. The results obtained from the analysis are in coherence with the requirements of a microwave filter.

Another S-band bandpass filter is proposed in this perspective where the performance achieved can be described in terms of fractional bandwidth around 30%, minimum return loss (64dB), maximum insertion loss (1.9dB) and a maximum group delay of 2ns. The footprint of the final design is 83X53$mm^{2,}$ which is relatively small as compared to other traditional S-band Microwave filters. The filter is fabricated and the S_{11} results are measured using the Vector Network analyzer (VNA) E5071C. Overall it can be considered to be a decent design for applications like satellite communication sub-systems and military radar. However the present size of these filters can be reduced by almost 50 percent by using Half-mode concept of Substrate Integrated waveguides, which is well detailed in the chapter 4.

Chapter 4

Design and Analysis of Compact HMSIW Filters

4.1 Introduction

In this chapter the HMSIW filter design process is discussed. To validate the concept and its features, two HMSIW bandpass filters are designed using the models proposed in chapter 3. These two filters are designed to work in X-band (8-12GHz) and Ku-band (GHz) of microwave frequencies. Simulation and parametric analysis of the designed filters are done using HFSS v.14.

4.2 Half-mode SIW filter theory

Half-mode SIW is a technique developed to reduce the size of the SIW device to almost half the actual size. The modes present in HMSIW, calculation of effective width of HMSIW and other theories related to this are described in chapter 2. So to design a HMSIW filter, the first thing needs to be calculated is the width of HMSIW. As given in chapter 2 HMSIW width is half the SIW effective width. The calculation of the required design parameters are done using the Equations (2.28)-(2.31) given in chapter 2.

4.3 Design of a compact Ku band HMSIW bandpass filter

A Ku-band SIW filter is proposed in chapter 3, which is very compact in size and decent in performance. However the size of it can be reduced further by using the HMSIW concept of filter design. The model proposed in chapter 3 for applications in Ku-band is used as a base for designing its equivalent HMSIW model. The designed filter uses a low-cost substrate FR4.

4.3.1 Design calculations

The design dimensions are calculated according to:

- The center frequency in the passband of the filter. which is 15GHz for Ku-band (12-18GHz).
- The cutoff frequency of the filter, which is 11.5GHz for Ku-band.

- The guided wavelength of the filter, which is responsible for the feed line width calculation.

The relation between the effective width of HMSIW and cutoff frequency of the dominant mode in the guide can be written in the following equation:

$$f_{cTE0.5,0} = \frac{c}{4W_{eff,HMSIW}\sqrt{\varepsilon_r}} \tag{4.1}$$

Except this cutoff frequency, other calculations are made according to the theory of SIW filter design as given in chapter 3.

4.3.2 Structure and dimensions

The structure looks similar to the half of SIW as shown in Figure 4.1. This structure is made using tapered-via feeding and basic EBG structures proposed in chapter3. The dimensions are calculated using Equations given in chapter 2. Some of the important dimensions like width of HMSIW $W_{eff,HMSIW}$, length of taper l_{tap} , width of taper, width of feed and total size of the model (w X H) are given in Table 4.1. Since the field-profile and cutoff frequency of the dominant mode doesn't depend on the height of the substrate, the thickness of the substrate taken is 0.5mm for the design.

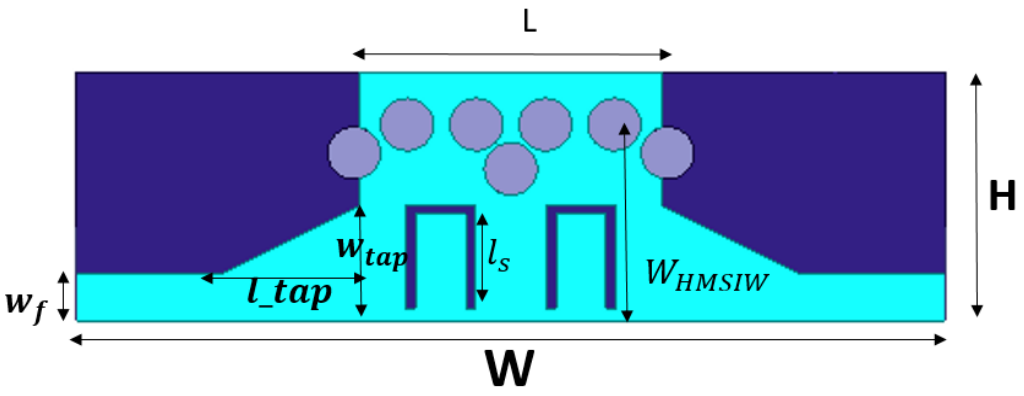

Figure 4.1: Top view of the Ku-band HMSIW filter structure

Table 4.1: Design dimensions of the Ku-band HMSIW Filter

Design parameters (in mm)	**Proposed Design**
W_{HMSIW}	4
w	17.4
l_{tap}	4
w_{tap}	2.2
l_s	1.98
H	5

4.3.3 Results and analysis

The filter as shown in Figure 4.1 is designed and simulated using HFSS. The S-parameter results and group delay of the filter are described in the following sections.

(i) Scattering parameter curves

The insertion loss and return loss curves are shown in the Figure 4.2. It can be deduced from the Figure 4.2 that the insertion loss is around 1.5dB which is very close the value 1.4dB achieved in the SIW filter for the same band proposed in chapter 3.

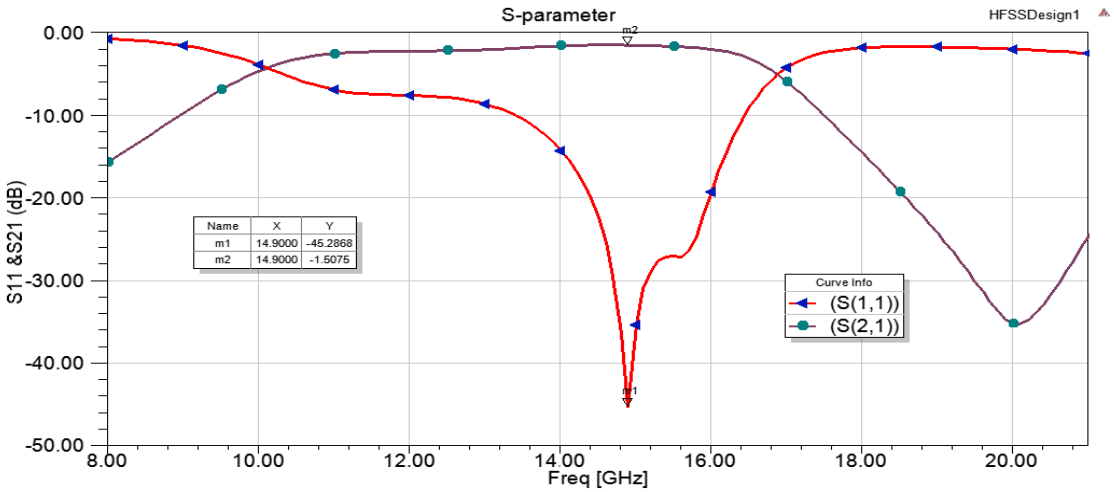

Figure 4.2: S-parameter curves of the HMSIW Ku-band filter

From the Figure 4.2 it's observed that the S_{11} is as low as -46dB at the frequency of 14.9GHz. It can also be seen that the upper stopband zero is having an insertion loss of 35dB at 20GHz.

(ii) Group delay

The group delay of a filter shows the linearity of the device in its operation band of frequencies. Group delay for the proposed filter comes-out to be linear and almost constant in the entire passband as shown in Figure 4.3. It can be seen from the Figure 4.3 that the group delay is very small and ranging from 0.15 to 0.25 nano sec in the passband.

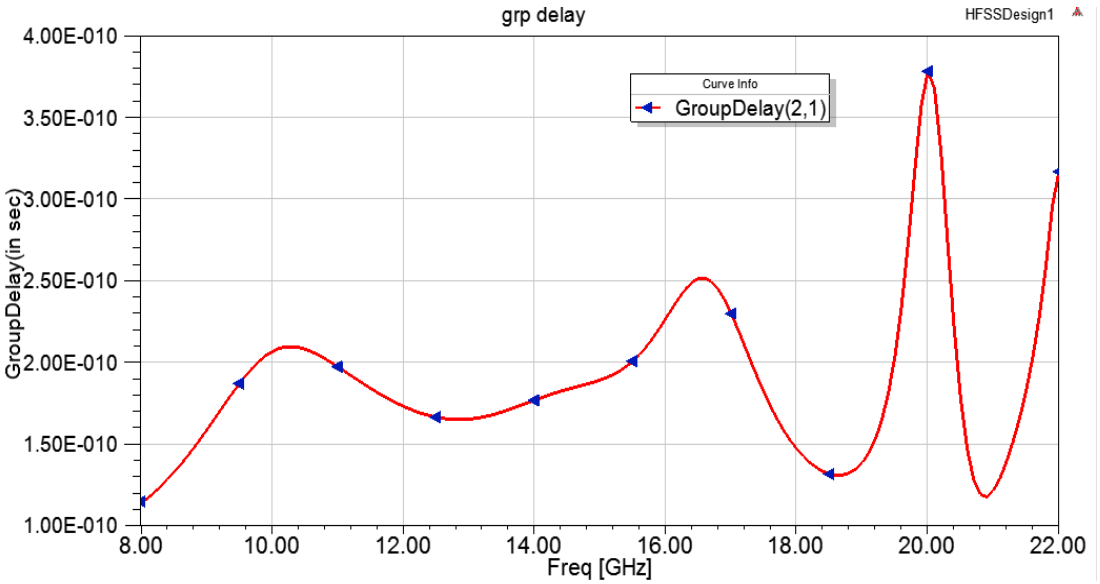

Figure 4.3: Group delay of the HMSIW Ku-band filter

The return loss is achieved as 45dB and insertion loss is 1.5dB in the passband of the filter which is quite good corresponding to the size. The footprint of the filter is 87mm^2 which is relatively small as compared to 160mm^2 of the filter given in chapter 3. However the bandwidth is little less than the SIW filter proposed in previous chapter.

4.4 Design of a compact X band HMSIW bandpass filter

X-band (8-12 GHz) has applications in mobile satellite, military radars and radio communication. For variant applications another bandpass filter is designed for x-band. The designed filter is then simulated using HFSS v.14.

4.4.1 Design calculations

The calculation of parameters are done using the equations and theory described in chapter 2. The design dimensions are calculated according to:

- The center frequency in the passband of the filter, which is 10GHz for X-band 8-12GHz).
- The cutoff frequency of the filter, which is 7GHz for X-band.

4.4.2 Structure and dimensions

The structure consists of two U-slots and a tapered-via feeding as shown in Figure 4.4 which is same as the previous design done for Ku-band applications. Dimensions of the design are calculated using equations described in chapter 2. Some of the important dimensions like width of HMSIW i.e. W_{HMSIW} , length of taper l_{tap} , width of taper , width of feed, distance between the two u-slots and total size of the model (w X H) are given in Table 4.2 . The design is made on a low-cost substrate FR4 having loss tangent (tanδ) of 0.02 and 0.5mm thickness.

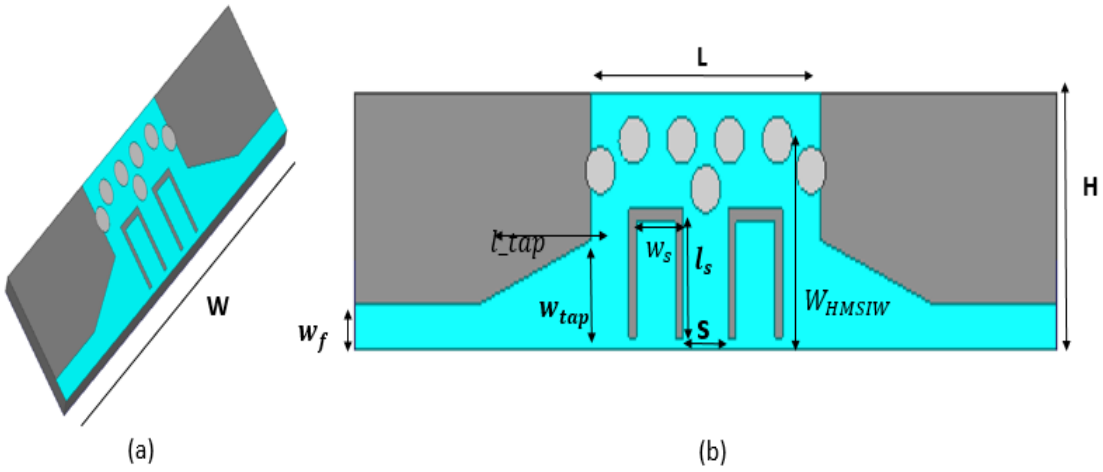

Figure 4.4: (a) Diametric view of the designed x-band HMSIW filter (b) Top-view of the HMSIW filter

Table 4.2: Design dimensions of the X-band HMSIW Filter

Design parameters (in mm)	Proposed Design
W_{HMSIW}	4.46
w	23.2
l_{tap}	3.85
w_{tap}	2.34
l_s	2.75
H	5.46
s	1.48
wf	0.9584

4.4.3 Results and analysis

The structure given in Figure 4.4 is designed and simulated using HFSS, and the obtained results are discussed in the following section.

(i) S-parameter curves

The simulated results for S_{11} and S_{21} are shown in Figure 4.5.

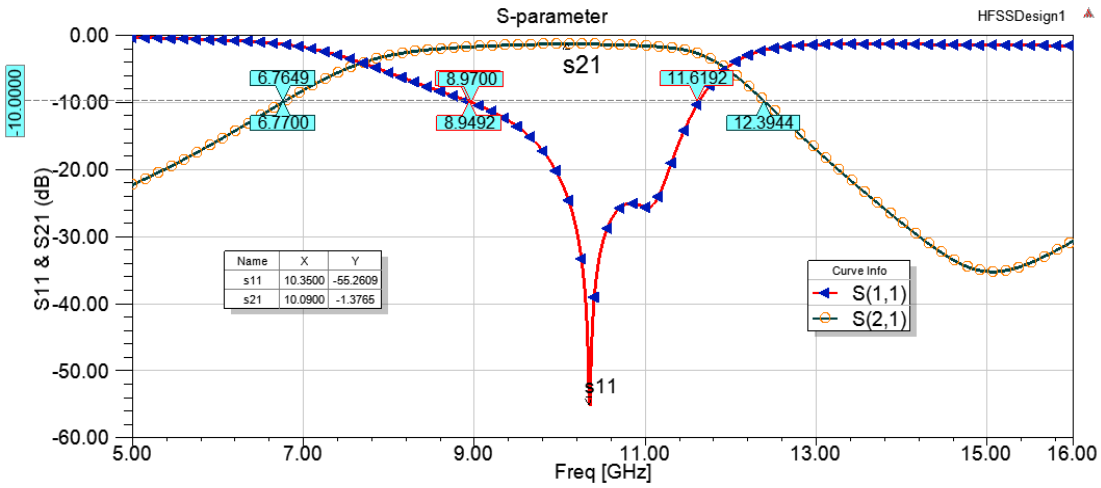

Figure 4.5: S-parameter curves of the HMSIW Ku-band filter

The return loss is achieved as 55dB at a frequency of 10.36GHz which is quite good as compared to the traditional SIW filters for X-band. The insertion loss is found out to be

1.37dB in the passband and around 35dB at the upper-stopband. The upper-stopband zero is formed due to the use of EBG structure i.e. U-slots. The bandwidth is around 1.8GHz ranging from 8.97GHz to 11.6GHz.

(ii) Group delay

Group delay vs. frequency has been plotted to verify the linearity of the filter. The curve shows almost a constant value of 0.3nano sec in the entire passband of the filter as shown in Figure 4.6.

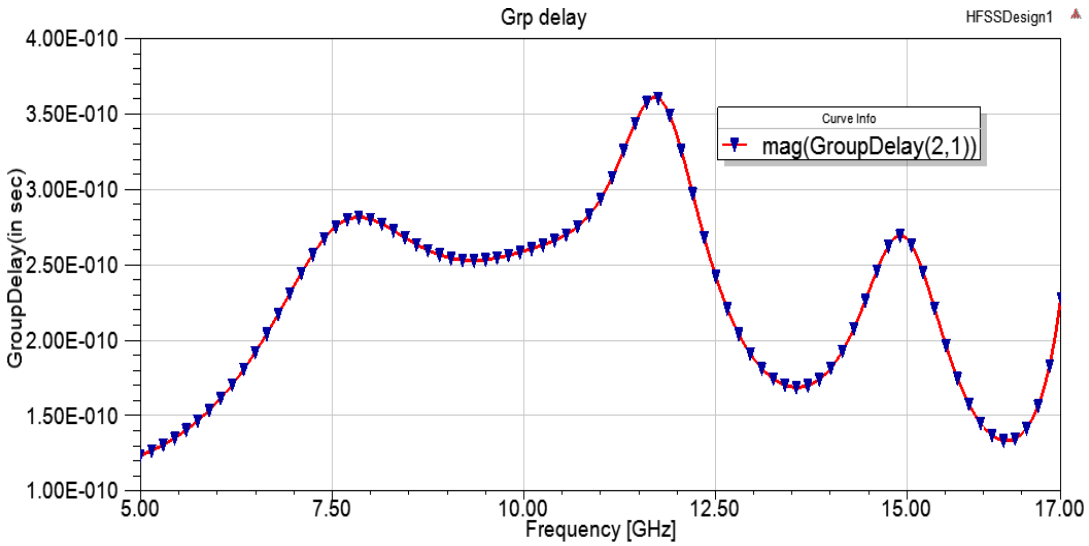

Figure 4.6: Group delay of the X-band HMSIW filter

4.5 Summary

In this chapter two HMSIW bandpass filters are investigated, one for the X-band and another for the Ku-band applications. The filters are designed and simulated using HFSS. The results obtained are discussed using different plots like scattering curves and group delay plot for the filters. The size reduction of almost 50% is achieved using the half-mode technique for SIW filter design. A compact HMSIW bandpass filter is designed for the Ku-band applications which is almost half in size as compared to conventional SIW designs as proposed in chapter 3. Another compact HMSIW bandpass filter is designed for X-band using low-cost substrate FR-4 whose size is almost half as compared to conventional SIW designs. The return loss is achieved as 55dB and insertion loss is 1.37dB in the passband of the filter which is quite good corresponding to the compactness. The overall footprint of the filter is 102mm^2 which is half of the equivalent SIW filter.

Chapter 5

Conclusions and Future scope

5.1 Conclusions

In this thesis the design and analysis of SIW filters with high isolation, better compactness and improved return loss has been discussed. The major contributions are outlined as follows:

- A compact and improved Ku-band bandpass filter with a smooth planar microstrip to SIW transition having multiple 'U'-slots is presented in chapter 3. The proposed design possesses better stop-band characteristics and provides high isolation of 1.4dB in the pass band. The SIW structure introduces transmission zeros in the upper stopband region of the filter. The taper-via transition at the planar to SIW provides lower reflection which results in wide bandwidth of the filter. The overall is 160 mm^2 which displays shows compactness.
- Another similar filter is designed for S-band (2-4GHz) to understand the behavior in the lower frequency bands. The design of the filter is given in chapter 3. The filter is fabricated using FR4 and measured results of S_{11} are quite decent as compared to simulation results. Return loss of the fabricated filter is achieved as low as 30dB in the passband region. The simulation performance achieved can be described in terms of fractional bandwidth which is 30%, lowest return loss (64dB), maximum insertion loss (1.9dB) and a maximum group delay of 2 nano sec.
- A HMSIW bandpass filter is designed for the Ku-band applications as presented in chapter 4. The proposed design is almost half in size as compared to conventional SIW designs as given in chapter 3. The return loss is achieved as 45dB and insertion loss 1.5dB in the passband of the filter which is quite good corresponding to the size. The footprint of the filter is $87mm^2$ which is relatively small as compared to $160mm^2$ filter presented in chapter 3.
- Another X-band filter is designed using HMSIW technique proposed in chapter 4.the size of this is almost half as compared to conventional SIW designs. The return loss is achieved as 55dB and insertion loss is 1.37dB in the passband of the filter which is quite good corresponding to the compactness. The overall footprint of the filter is $102mm^2$ which is half of the equivalent SIW filter.

5.2 Future scope

The designed filters can be modified by using movable metallic vias and micro electro-mechanical switches (MEMS) to design frequency reconfigurable filters. The future scope of this work can be briefed as follows:

- Use of movable via for tunable SIW filter design to have applications in different ITU (International Telecom Unit) regions of Ku-band.
- Use of different switches like PIN diodes, SPDT and MEMS to design frequency reconfigurable filters.

References

[1] Matthaei, G. L., Young, L., & Jones, E. M. T. (1964). *Microwave filters, impedance-matching networks, and coupling structures* (Vol. 1). Artech house.

[2] Hunter, Ian: *'Theory and Design of Microwave Filters*', IET electromagnetic waves series 48, 2001.

[3] Hong, J.S.G. and Lancaster, M.J., 2004. *Microstrip filters for RF/microwave applications* (Vol. 167). John Wiley & Sons.

[4] Pozar, David M. "*Microwave engineering"*. John Wiley & Sons, 2009.

[5] *Ke Wu, D. Deslandes and Y. Cassivi, "The substrate integrated circuits – a new concept for high-frequency electronics and optoelectronics,"* Telecommunications in Modern Satellite, Cable and Broadcasting Service, 2003. TELSIKS 2003. 6th International Conference on, *2003, pp. P-III-P-X vol.1.*

[6] *S. S. Sabri, B. H. Ahmad and A. R. B. Othman, "A review of Substrate Integrated Waveguide (SIW) bandpass filter based on different methods and design,"* Applied Electromagnetics (APACE), 2012 IEEE Asia-Pacific Conference on, *Melaka, 2012, pp. 210-215.*

[7] Z. Kordiboroujeni and J. Bornemann, "Designing the Width of Substrate Integrated Waveguide Structures," *IEEE Microwave and Wireless Components Letters*, vol. 23, no. 10, pp. 518-520, Oct. 2013.

[8] *Z. Kordiboroujeni and J. Bornemann, "New Wideband Transition From Microstrip Line to Substrate Integrated Waveguide," in* IEEE Transactions on Microwave Theory and Techniques, *vol. 62, no. 12, pp. 2983-2989, Dec. 2014*

[9] S. W. Wong, R. S. Chen, K. Wang, Z. N. Chen and Q. X. Chu, "U-Shape Slots Structure on Substrate Integrated Waveguide for 40-GHz Bandpass Filter Using LTCC Technology," in IEEE Transactions on Components, Packaging and Manufacturing Technology, vol. 5, no. 1, pp. 128-134, Jan. 2015.

[10] R. S. Chen, S. W. Wong, L. Zhu and Q. X. Chu, "Wideband Bandpass Filter Using U-Slotted Substrate Integrated Waveguide (SIW) Cavities," IEEE Microwave and Wireless Components Letters, vol. 25, no. 1, pp. 1-3, Jan. 2015.

[11] Rui-Sen Chen, Sai Wai Wong, Zai-Cheng Guo, Kai Wang and Qin-Xin Chu, "Wideband bandpass filter based on substrate integrated waveguide (SIW) and half-mode substrate integrated waveguide (HMSIW) cavities," Wireless Symposium (IWS), 2015 IEEE International, Shenzhen, 2015, pp. 1-4.

[12] Feng Xu and Ke Wu, "Guided-wave and leakage characteristics of substrate integrated waveguide," in IEEE Transactions on Microwave Theory and Techniques, vol. 53, no. 1, pp. 66-73, Jan. 2005.

[13] D. Deslandes and Ke Wu, "Accurate modeling, wave mechanisms, and design considerations of a substrate integrated waveguide," in IEEE Transactions on Microwave Theory and Techniques, vol. 54, no. 6, pp. 2516-2526, June 2006.

[14] D. Deslandes and K. Wu, "Design Consideration and Performance Analysis of Substrate Integrated Waveguide Components," Microwave Conference, 2002. 32nd European, Milan, Italy, 2002, pp. 1-4.

[15] Y. Cassivi, L. Perregrini, P. Arcioni, M. Bressan, K. Wu, and G. Conciauro, "Dispersion characteristics of substrate integrated rectangular waveguide," IEEE Microw. Wireless. Compon. Lett., vol. 12, pp. 333-335, Sep. 2002.

[16] D. Deslandes and K. Wu, "Integrated microstrip and rectangular waveguide in planar form," in IEEE Microwave and Wireless Components Letters, vol. 11, no. 2, pp. 68-70, Feb. 2001.

[17] D. Deslandes and Ke Wu, "Integrated transition of coplanar to rectangular waveguides," Microwave Symposium Digest, 2001 IEEE MTT-S International, Phoenix, AZ, USA, 2001, pp. 619-622 vol.2.

[18] W. Hong et al., "Half Mode Substrate Integrated Waveguide: A New Guided Wave Structure for Microwave and Millimeter Wave Application," 2006 Joint 31st International Conference on Infrared Millimeter Waves and 14th International Conference on Teraherz Electronics, Shanghai, 2006, pp. 219-219.

[19] Q. H. Lai, C. Fumeaux, W. Hong, and R. Vahldieck, "Characterization of the propagation properties of the half-mode substrate integrated waveguide," IEEE Trans. Microw. Theory Tech., vol. 57, pp. 1996-2004, Aug. 2009.

[20] D. L. Diedhiou, E. Rius, J. F. Favennec and A. El Mostrah, "Ku-Band Cross-Coupled Ceramic SIW Filter Using a Novel Electric Cross-Coupling," IEEE Microwave and Wireless Components Letters, vol. 25, no. 2, pp. 109-111, Feb. 2015.

[21] S. Moitra, B. Mondal, J. Kundu, A. K. Mukhopadhyay and A. K. Bhattacharjee, "Substrate Integrated Waveguide (SIW) filter using stepped-inductive posts for Ku-band applications,"Computational Intelligence and Information Technology, 2013. CIIT 2013. Third International Conference on, Mumbai, 2013, pp. 398-401.

[22] C S Panda , R Nayak, S K Behera "*Design and Analysis of a Compact Substrate Integrated Waveguide Bandpass Filter for Ku Band Applications*" IEEE International Conference on Innovations in information Embedded and Communication Systems (ICIIECS16), Coimbatore, Tamilnadu, India, 17-18 March 2016.

Bibliography

- Huang, Liwen (2013) "*Novel substrate integrated waveguide filters and circuits".* PhD thesis, University of Leeds.
- A. Boutejdar, A. Batmanov, M. H. Awida, E. P. Burte and A. Omar, "Design of a new bandpass filter with sharp transition band using multilayer-technique and U-defected ground structure," in *IET Microwaves, Antennas & Propagation*, vol. 4, no. 9, pp. 1415-1420, September 2010.
- T. R. Jones and M. Daneshmand, "A new type of capacitively-loaded half-mode substrate integrated waveguide for miniaturized guided wave applications," *2015 IEEE MTT-S International Microwave Symposium*, Phoenix, AZ, 2015, pp. 1-4.
- . W. Wong, K. Wang, Z. N. Chen and Q. X. Chu, "Design of Millimeter-Wave Bandpass Filter Using Electric Coupling of Substrate Integrated Waveguide (SIW)," in *IEEE Microwave and Wireless Components Letters*, vol. 24, no. 1, pp. 26-28, Jan. 2014.
- A. Genc, R. Baktur and R. J. Jost, "Dual-Bandpass Filters With Individually Controllable Passbands," in *IEEE Transactions on Components, Packaging and Manufacturing Technology*, vol. 3, no. 1, pp. 105-112, Jan. 2013.
- C. T. Bui, P. Lorenz, M. Saglam, W. Kraemer and R. H. Jansen, "Investigation of Symmetry Influence in Substrate Integrated Waveguide (SIW) Band-Pass Filters using Symmetric Inductive Posts," *Microwave Conference, 2008. EuMC 2008. 38th European*, Amsterdam, 2008, pp. 492-495.
- W. Hong and K. Gong, "Miniaturization of substrate integrated bandpass filters," *2010 Asia-Pacific Microwave Conference*, Yokohama, 2010, pp. 247-250.
- M. Z. Ur Rehman, Z. Baharudin, M. A. Zakariya, M. H. M. Khir, M. T. Khan and P. W. Weng, "Recent advances in miniaturization of Substrate integrated waveguide bandpass filters and its applications in tunable filters," *Business Engineering and Industrial Applications Colloquium (BEIAC), 2013 IEEE*, Langkawi, 2013, pp. 109-114.
- G. Gentile, B. Rejaei, V. Jovanović, L. K. Nanver, L. C. N. de Vreede and M. Spirito, "Ultra-wide band CPW to substrate integrated waveguide (SIW) transition based on a U-shaped slot antenna," *Microwave Integrated Circuits Conference (EuMIC), 2013 European*, Nuremberg, 2013, pp. 25-28.

Dissemination

- C S Panda , R Nayak, S K Behera "*Design and Analysis of a Compact Substrate Integrated Waveguide Bandpass Filter for Ku Band Applications*" IEEE International Conference on Innovations in information Embedded and Communication Systems (ICIIECS16), Coimbatore, Tamilnadu , India, 17-18 March 2016.